



OASIS-3: IMAGING METHODS AND DATA DICTIONARY

VERSION 2.2 JULY 2022



CONTENTS

| | |
|---|----|
| Version 2.2 July 2022 | 1 |
| Introduction & Contact Information..... | 5 |
| Access to OASIS-3 | 5 |
| Data Use Agreement..... | 6 |
| OASIS Projects and Citations | 7 |
| Data Releases..... | 7 |
| Release 1.0: March 2018 | 7 |
| Release 1.2: April 2018 | 7 |
| Release 2.0: July 2022..... | 7 |
| Change Log Records..... | 8 |
| Using Central.XNAT.ORG | 8 |
| Github Resources..... | 9 |
| Data scripts: Download and Session Matching | 9 |
| Demographics | 11 |
| Table 1-2. Subject Demographics | 11 |
| OASIS File Description..... | 11 |
| MR Images | 12 |
| PET Images..... | 12 |
| Tables 3-6. OASIS-3 Imaging Summary..... | 13 |
| Figure 1 Longitudinal Imaging..... | 14 |
| MR Imaging..... | 15 |
| MR Scanners | 15 |
| Scanning Methods | 15 |
| DTI Imaging | 15 |
| Resting State SCans – Slice Timing..... | 16 |
| ASL Parameters..... | 16 |

| | |
|---|----|
| Post-Processed MRI: Volumetric Segmentation | 16 |
| Freesurfer | 16 |
| Processing Background | 17 |
| Quality Control MEasures | 17 |
| Analysis Considerations | 17 |
| Correcting subcortical and cortical volumes for head size | 18 |
| Instructions for normalization of MRI freesurfer-derived cortical volumes | 18 |
| Additional Regional Calculations | 19 |
| MR Scanner Comperison: Siemens TIM Trio 3T and Siemens Biograph 3T mMR | 19 |
| PET Imaging | 21 |
| PET Scanners | 21 |
| HR+ Image Notes (PIB and FDG) | 21 |
| Tracers | 21 |
| PIB | 21 |
| AV45 | 21 |
| FDG | 22 |
| AV1451 | 22 |
| Post-Processed PET: Pet Unified Pipeline (PUP) | 22 |
| PUP Variable Nomenclature | 23 |
| Partial Volume Correction | 23 |
| Alternative Reference Region | 24 |
| Amyloid PET Imaging Analysis | 24 |
| Cutoff Values for Amyloid Positivity | 25 |
| Centiloid Conversion for Amyloid PET | 26 |
| Tau PET Imaging (OASIS3_AV1451) | 28 |
| Braak Staging | 28 |
| Cutoff Values for Tau Positivity | 29 |

| | |
|----------------------------|----|
| Freesurfer Variables | 30 |
| PUP Variables..... | 33 |
| References..... | 38 |

INTRODUCTION & CONTACT INFORMATION

OASIS-3 is the latest release in the *Open Access Series of Imaging Studies (OASIS)* that aimed at making neuroimaging datasets freely available to the scientific community. By compiling and freely distributing this multi-modal dataset, we hope to facilitate future discoveries in basic and clinical neuroscience. Previously released data for OASIS-Cross-sectional (Marcus et al, 2007) and OASIS-Longitudinal (Marcus et al, 2010) have been utilized for hypothesis driven data analyses, development of neuroanatomical atlases, and development of segmentation algorithms. OASIS-3 is a longitudinal neuroimaging, clinical, cognitive, and biomarker dataset for normal aging and Alzheimer's Disease.

The OASIS datasets hosted by central.xnat.org provide the community with open access to a significant database of neuroimaging and processed imaging data across a broad demographic, cognitive, and genetic spectrum an easily accessible platform for use in neuroimaging, clinical, and cognitive research on normal aging and cognitive decline. All data is available via www.oasis-brains.org.

OASIS-3 is a retrospective compilation of data for 1378 participants that were collected across several ongoing projects through the WUSTL Knight ADRC over the course of 30 years. Participants include 755 cognitively normal adults and 622 individuals at various stages of cognitive decline ranging in age from 42-95 yrs. All participants were assigned a new random identifier and all dates were removed and normalized to reflect days from entry into study. The dataset contains 2842 MR sessions which include T1w, T2w, FLAIR, ASL, SWI, time of flight, resting-state BOLD, and DTI sequences. Many of the MR sessions are accompanied by volumetric segmentation files produced through Freesurfer processing. PET imaging from different tracers, PIB, AV45, and FDG, totaling over 2157 raw imaging scans and the accompanying post-processed files from the Pet Unified Pipeline (PUP) are also available in OASIS-3. Additionally, 451 Tau PET sessions and post-processed PUP are now available for OASIS-3 subjects in a subproject 'OASIS-3_AV1451'.

ACCESS TO OASIS-3

Access to OASIS imaging, clinical, and biomarker data is available for access after completing the Data Use Agreement. Please log all data access requests using the online forms at www.oasis-brains.org.

- Data is available for access at <https://central.xnat.org>
- Further resources, including updated copies of this Data Dictionary, are available online at www.oasis-brains.org.
- Both OASIS-1 (OASIS: Cross-Sectional) and OASIS-2 (OASIS: Longitudinal) are available at www.oasis-brains.org/#data.
- CONTACT INFORMATION: oasis-brains@nrg.wustl.edu

DATA USE AGREEMENT

The OASIS data are distributed to the greater scientific community under the following terms:

1. You will not attempt to establish the identity of or make contact with any of the included human participants.
2. You will acknowledge the use of OASIS data and data derived from OASIS data when publicly presenting any results or algorithms that benefitted from their use. Papers, book chapters, books, posters, oral presentations, and all other printed and digital presentations of results derived from OASIS data should contain the following:
 - a. Acknowledgments: "Data were provided [in part] by OASIS [insert appropriate OASIS source info]"
 - i. OASIS: Cross-Sectional: Principal Investigators: D. Marcus, R. Buckner, J. Csernansky, J. Morris; P50 AG05681, P01 AG03991, P01 AG026276, R01 AG021910, P20 MH071616, U24 RR021382
 - ii. OASIS: Longitudinal: Principal Investigators: D. Marcus, R. Buckner, J. Csernansky, J. Morris; P50 AG05681, P01 AG03991, P01 AG026276, R01 AG021910, P20 MH071616, U24 RR021382
 - iii. OASIS-3: Longitudinal Multimodal Neuroimaging: Principal Investigators: T. Benzinger, D. Marcus, J. Morris; NIH P50 AG00561, P30 NS09857781, P01 AG026276, P01 AG003991, R01 AG043434, UL1 TR000448, R01 EB009352. AV-45 doses were provided by Avid Radiopharmaceuticals, a wholly owned subsidiary of Eli Lilly.
 - iv. OASIS-3 AV1451: Principal Investigators: T. Benzinger, J. Morris; AW00006993. AV-1451 doses were provided by Avid Radiopharmaceuticals, a wholly owned subsidiary of Eli Lilly.
 - v. OASIS-4: Clinical Cohort: Principal Investigators: T. Benzinger, L. Koenig, P. LaMontagne
 - b. Citation: The specific publications that are appropriate to cite in any given study will depend on what OASIS data were used and for what purposes. An annotated and current list of OASIS publications is available at <http://www.oasis-brains.org>.
 - i. OASIS: Cross-Sectional: <https://doi.org/10.1162/jocn.2007.19.9.1498>
 - ii. OASIS: Longitudinal: <https://doi.org/10.1162/jocn.2009.21407>
 - iii. OASIS-3: Longitudinal Multimodal Neuroimaging: <https://doi.org/10.1101/2019.12.13.19014902>
 - iv. OASIS-4: Clinical Cohort: <https://doi.org/10.1016/j.nicl.2020.102248>
 - c. All proposed publications or presentations using Flortbetapir F18 (AV45) and Flortaucipir F18 (AV1451) PET data must be submitted to Avid Radiopharmaceuticals for review and comment thirty days prior to such presentation or publication for review of intellectual property interests. See below for contact information and details.
3. You agree to provide the Knight ADRC upon request with information on your use of OASIS data
4. Failure to abide by these data use terms may result in termination of your right to access and use OASIS data.

AVID CONTACT INFO FOR FLORBETAPIR (AV45) PRESENTATIONS AND PUBLICATIONS

All proposed publications or presentations using Flortbetapir F18 (AV45) or Flortaucipir F18 (AV1451) PET data must be submitted to Avid Radiopharmaceuticals for review and comment 30 days prior to such presentation or publication for review of intellectual property interests. Please reference OASIS-brains.org and Washington University (Drs. Morris and Benzinger) in your email.

- Contacts:
 - o Patricia Aldea Stevenson <stevenson@lilly.com>

OASIS PROJECTS AND CITATIONS

Each OASIS project should be used independently and not combined. Due to anonymization participants may be included in all three datasets (OASIS-1, OASIS-2, and OASIS-3) under unique IDs.

- OASIS-1: Cross-Sectional T1w MR images across the lifespan (ages 18-96) with dementia status (doi: [10.1162/jocn.2007.19.9.1498](https://doi.org/10.1162/jocn.2007.19.9.1498))
- OASIS-2: Longitudinal T1w MR images in older adults (ages 60-96) with dementia status (doi: [10.1162/jocn.2009.21407](https://doi.org/10.1162/jocn.2009.21407))
- OASIS-3: Longitudinal Multimodal Neuroimaging (ages 42-95) with dementia status ([doi.org: 10.1101/2019.12.13.19014902](https://doi.org/10.1101/2019.12.13.19014902))
- OASIS-4: Clinical Cohort: <https://doi.org/10.1016/j.nicl.2020.102248>

DATA RELEASES

RELEASE 1.0: MARCH 2018

Initial Longitudinal release of data

- 1098 Subjects (age 42-95)
- Neuroimaging:
 - 2118 MR Sessions
 - 1912 Freesurfer processed outputs
- Clinical and Cognitive Measures:
 - 6534 Longitudinal Clinical follow-up assessments
 - Neuropsych Assessments
 - 4089 NACC UDS2 Assessments

RELEASE 1.2: APRIL 2018

- 1435 PET Sessions
 - 1352 PET Unified Pipeline processed outputs

RELEASE 2.0: JULY 2022

Updated longitudinal data to existing subjects and addition of new subjects.

- **New subjects and longitudinal session**
 - 280 Subjects (age 42-100)
 - Neuroimaging:

- 674 MR Sessions
 - 633 Freesurfer processed outputs
- 1472 CT session
- 550 PET Sessions
 - 493 PET Unified Pipeline processed outputs
- **Spreadsheets for download without using xnat tables**
- **UDS v2 and UDS v3**
- **Cohort Replication**
 - Option for storage of cohort data to replicate published results
- **OASIS3_AV1451**
 - Sub-project with Tau imaging on OASIS3 participants

CHANGE LOG RECORDS

- This is a changelog to track changes to the OASIS database.
 - https://github.com/NrgXnat/oasis-scripts/blob/master/OASIS_CHANGELOG.md

USING CENTRAL.XNAT.ORG

SEARCHING, REPORTING, AND DATA MINING:

- **Standard Search:** <https://wiki.xnat.org/documentation/how-to-use-xnat/using-the-standard-search>
- **Using the Advanced Search:** <https://wiki.xnat.org/documentation/how-to-use-xnat/using-the-standard-search/using-the-advanced-search>
- **Saving a Data Table as a Stored Search:** <https://wiki.xnat.org/documentation/how-to-use-xnat/using-the-standard-search/saving-a-data-table-as-a-stored-search>
- **How to Edit, Filter, and Join Tables:** <https://wiki.xnat.org/documentation/how-to-use-xnat/using-the-standard-search/how-to-edit-filter-and-join-data-tables>

DOWNLOADING DATA

- **How to Download Files via the XNAT REST API (*recommended*):**
<https://wiki.xnat.org/display/XAPI/How+To+Download+Files+via+the+XNAT+REST+API>
 - **Scripted Download Instructions:** The following shell script can be used to download large amounts of data from the OASIS-3 dataset on XNAT Central.
 - Create a CSV spreadsheet with a list of sessions to download (or download a CSV from XNAT Central)
 - Download the script: <https://github.com/NrgXnat/oasis-scripts>
 - Open a Terminal window (on Mac) or Command Line window (on PC / Linux)
 - To run the script and download data, you need to provide the following parameters:
 - <input_file.csv> - your list of sessions to download
 - <directory_name> - the path to your local download folder

- <xnat_central_username> - your username
 - <scan_type> - (optional) the type of scan or scans to download
- **How to Download non-imaging assessments**
 - Subject “[OAS data files](#)” contains an MR session ([OASIS3 data files](#)) that has all csv files.
 - 1. click on MR session
 - 2. select assessments you want to download
 - 3. bulk action Download
 - This “MR session” includes files for:
 - Demographics
- **How to Download Images from UI:** <https://wiki.xnat.org/documentation/how-to-use-xnat/how-to-download-image-data-from-xnat-projects>
- **Troubleshooting XNAT Java Applet Issues:** <https://wiki.xnat.org/documentation/how-to-use-xnat/image-session-upload-methods-in-xnat/troubleshooting-xnat-java-applet-issues>
 - UDS v2 and UDS v3 assessments
 - Psychometric variables
 - Image processing outputs (freesurfer, PUP, Centiloid)
 - json summary files
 - Data dictionaries
 - Data use agreement

GITHUB RESOURCES

DATA SCRIPTS: DOWNLOAD AND SESSION MATCHING

[HTTPS://GITHUB.COM/NRGXNAT/OASIS-SCRIPTS](https://github.com/NrgXnat/OASIS-SCRIPTS)

DOWNLOAD SCANS

- This script downloads scans of a specified type and organizes the files.
 - https://github.com/NrgXnat/oasis-scripts#download_scansdownload_oasis_scanssh
- This script downloads scans from OASIS and organizes the files into Brain Imaging Data Structure (BIDS) format (See the [BIDS website](#) and the [BIDS file specification](#) for more details on the BIDS format).
 - <https://github.com/NrgXnat/oasis-scripts#downloading-mr-and-pet-scan-files-in-bids-format>

DOWNLOAD FREESURFER

- The scripts contained in the `freesurfer` folder can be used to download Freesurfer data and organize the files.
 - <https://github.com/NrgXnat/oasis-scripts#downloading-freesurfer-files>

DOWNLOAD PUP

- The scripts contained in the `pup` folder can be used to download PUP data and organize the files.
 - <https://github.com/NrgXnat/oasis-scripts#downloading-pet-unified-pipeline-pup-files>

SESSION MATCHUP

- This script takes in two OASIS-3 .csv formatted spreadsheets and matches up the sessions based on your requested days from entry distance requirements. This script requires R at least version 3.3.0 and the R `data.table` library minimum version 1.12.8. See the R-project website for more details on the R language and visit the R `data.table` library website for more details on the `data.table` library.

OASIS-3 data has been anonymized and dates have been eliminated from the data set. OASIS-3 instead uses "days from entry" to note when scan sessions and questionnaire sessions happen relative to each other. The "days from entry" variable is seen in OASIS-3 IDs for MR sessions, PET sessions, Freesurfer assessors, PUP assessors, and questionnaire sessions (such as ADRC Clinical Data entries or UDS form entries). At the end of each ID is a string `d0000` where `0000` is the days since the subject's entry date into the study. A days from entry value of 0 means that this is the subject's first visit.

- <https://github.com/NrgXnat/oasis-scripts#matching-up-session-data-by-days-from-entry>

DEMOGRAPHICS

TABLE 1-2. SUBJECT DEMOGRAPHICS

Table 1. Subject Demographics

| | N | AGE | Right Handed |
|-------|------|-------------------|--------------|
| F | 756 | 68.15 (43.2-95.6) | 684 |
| M | 622 | 70.16 (42.5-91.7) | 551 |
| Total | 1378 | 69.06 (42.5-95.6) | 1235 |

Table 2. OASIS-3 Clinical Dementia Rating (CDR) Summary

| | <i>max CDR</i> | | | | | |
|----------------|----------------|-----|-----|-----|----|-------------|
| <i>min CDR</i> | 0 | 0.5 | 1 | 2 | 3 | Grand Total |
| 0 | 755* | 215 | 61 | 38 | 7 | 1076 |
| 0.5 | | 83 | 57 | 74 | 7 | 221 |
| >1 | | | 33 | 36 | 5 | 74 |
| Grand Total | 755 | 298 | 151 | 154 | 19 | 1377 |

**Unchanged CDR = 0 represents cognitively healthy population. List provided on Central*

OASIS FILE DESCRIPTION

BIDS FILE SPECIFICATION

All MR and PET imaging files are converted to nifti format utilizing the BIDS format (Gorgolewski et al., 2016). This allows for standardized naming and file formats. Raw MR files, in DICOM or IMA format were converted to Nifti format using dcm2nii (DICOM=dcm2nii v1.0.20171017 and IMA=dcm2nii mricronlx64-2013.06.12; Li et al., 2016). In addition to nifti files, a supplemental json file is included with additional acquisition header information, such as TR, TE, flip angle, and scanner model, that is absent from nifti headers.

Documentation on BIDS can be found here (<http://bids.neuroimaging.io/>).

***Nifti conversion was completed after volumetric processing that has two big implications.**

- First, any new processing of T1 images through Freesurfer will result in different values as documented in FreeSurfer regarding file format changes.
- Second, the T1.mgz associated with the OASIS-3 Freesurfer processing is the result of dicom conversion to mgz and can be used in place of the T1w.nii file for comparative FreeSurfer processing.**

MR IMAGES

- anat
 - T1w
 - T2w
 - TSE (acq-TSE_T2w)
 - T2star
 - FLASH
 - Flair
 - Time of Flight (acq-TOF_angio)
- func
 - Task-rest_bold
 - ASL
- fmap
 - Fieldmap
- dwi
 - DWI
 - bvec (vector table)
 - bval (vector of b-values)
- swi
 - Magnitude (part-Mag_GRE)
 - Phase (part-Phase_GRE)
 - Minimum Intensity Projection (minIP)
 - SWI

PET IMAGES

- pet
 - acq-PIB_pet
 - acq-AV45_pet
 - acq-FDG_pet
 - acq-AV1451_pet* (*only in project: OASIS3_AV1451)

TABLES 3-6. OASIS-3 IMAGING SUMMARY

Table 3. OASIS-3 MR and PET Imaging Summary

| OASIS-3 – Longitudinal Normal Aging and Alzheimer Disease | | | | | | | | | | |
|--|----------|------|-----------|------|------|------|------|-----|--------|------|
| | Subjects | MR | Freesufer | CT | PET | AV45 | PIB | FDG | AV1451 | PUP |
| 2018 Release | 1098 | 2168 | 1912 | 0 | 1607 | 491 | 999 | 117 | | 1352 |
| 2022 Release | 281 | 674 | 633 | 1472 | 550 | 290 | 250 | 10 | | 493 |
| Total OASIS-3 | 1379 | 2842 | 2545 | 1472 | 2157 | 781 | 1249 | 127 | | 1845 |
| | | | | | | | | | | |
| OASIS3_AV1451 (restricted access) | 451 | | | | | | | | 449 | 434 |
| OASIS3_AV1451_longitudinal (restricted access – WUSTL ADRC only) | 79 | | | | | | | | 81 | 72 |

Table 4. OASIS-3 MR Scan Type Inventory

| Scan Type | T1w | T2w | FLAIR | Bold – Resting State | DTI | ASL | SWI | TOF | Fieldmap |
|---------------------------|------|------|-------|----------------------------|------|------|------|-----|----------|
| OASIS-3 | | | | | | | | | |
| 1.5T MR | 654 | 455 | 0 | 2 | 0 | 0 | 2 | 1 | 2 |
| 3.0T MR (Release 2018) | 2734 | 3145 | 748 | 3640 | 2450 | 1113 | 1217 | 674 | 2922 |
| 3.0T MR (Release 2022) | 728 | 450 | 633 | 1474 | 819 | 447 | 12 | 222 | 895 |
| | | | | | | | | | |
| OASIS-4 | 1846 | 769 | 671 | 10 | 656 | 1 | 663 | 18 | 3 |

| OASIS-3 – Longitudinal Normal Aging and Alzheimer Disease | | | | | | | |
|---|--------------|--------|--------|--------------|--------|--------|-------|
| | Release 2018 | | | Release 2022 | | | Total |
| | HR+ | PET/CT | PET/MR | HR+ | PET/CT | PET/MR | |
| | PIB | 411 | 580 | 8 | 11 | 239 | 1249 |
| | AV45 | 1 | 23 | 467 | 2 | 288 | 781 |
| | FDG | 117 | | | 10 | | 127 |
| Total | 529 | 603 | 475 | 23 | 239 | 288 | |

Table 5. PET imaging inventory by scanner and tracer

Table 6. Post-processing Data Summary

| | Post-Processed Data (Release 2018) | Post-Processed Data (Release 2022) |
|-------------------|---------------------------------------|---------------------------------------|
| FreeSurfer | | |
| 5.0/5.1 | 211 | 0 |
| 5.3 | 1701 | 633 |
| PUP | 1352 | 493 |
| PIB | 935 | 228 |
| AV45 | 417 | 265 |
| FDG | 0 | 0 |

FIGURE 1 LONGITUDINAL IMAGING

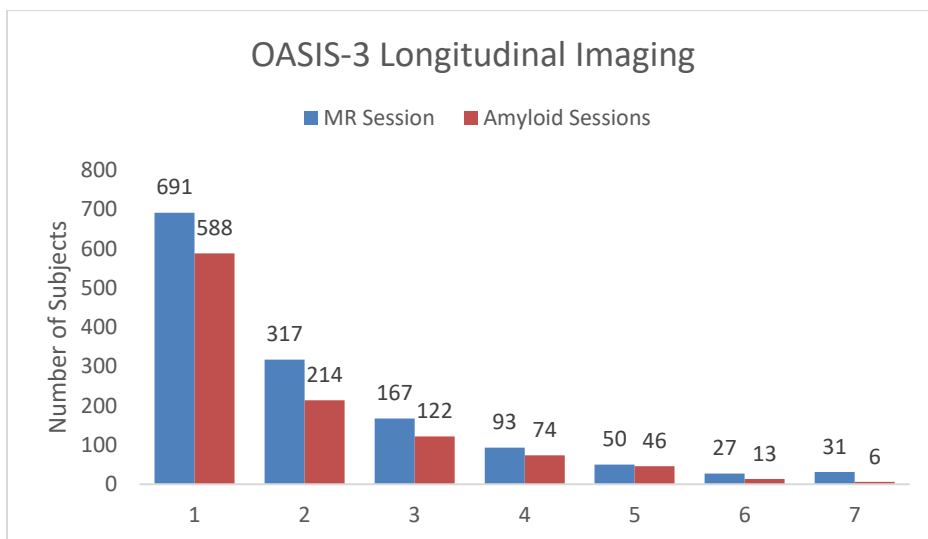


Figure 1. Longitudinal Imaging

MR IMAGING

MR SCANNERS

Data included in OASIS was collected on the following scanners. Scanner specific information is recorded in dataset_description.json for each MR scan session. *For manuscripts, select only the scanner(s) from which your subset of data were derived.*

- Siemens BioGraph mMR PET-MR 3T scanner (51010)
- Siemens TIM Trio 3T MR scanner (2 scanners) (35177 & 35248)
- Siemens Magnetom Vida 3T MR scanner (175614)
- Siemens Prisma_fit 3T MRI scanner (167047)
- Siemens Sonata 1.5T scanner (21926)
- Siemens Vision 1.5T scanner
- Siemens Avanto 1.5T scanner (26321)

SCANNING METHODS

- Participants were placed in the scanner head to foot while lying in the supine position.
- Head immobilization was done by placing small foam cushions between the head and the head coil.
- In many participants, a Vitamin E capsule was used to mark the left temple.
- For all scans a 16-channel head coil was used.
- Participants receiving simultaneous PET acquisition, on the BioGraph mMR were injected with tracer prior to initiation of MRI scanning
- Magnetom Vida scan sessions were converted to NIFTI format from enhanced DICOM format
- *Note that not all subjects will have every type of image data.*

DTI IMAGING

The OASIS-3 dataset includes 1205 DTI. All sequences include a *bvec and *bval file that includes information on the vectors and b-values as estimated through the dcm2niix conversion. These files are found in the BIDS folder associated with the DTI nifti. DTI sequences collected on Siemens scanners are known to have a variance of +/- 10%. Below is the standard vector table for Siemens 25-direction DTI.

VECTOR TABLE FOR 25 DIRECTIONS

CoordinateSystem = xyz

Normalisation = none

25 direction

0,1,2,3,4,5,6,7,8,9,10,11,12,13,14,15,16,17,18,19,20,21,22,23,24

-0.200000,-0.457663,-0.619678,-0.647200,-0.529196,-0.163313,-0.305531,-0.346410,-0.294225,-0.334708,-0.876353,-0.107041,-0.174797,-
0.222823,0.000000,0.000000,0.000000,0.000000,0.231234,0.435890,0.489898,0.223607,0.365180,0.626649,0.723592,0.809004
0.000000,0.000000,0.000000,-0.420560,-0.529196,0.163313,0.305531,0.589382,-0.770361,0,-0.294691,0.000000,0.000000,-0.446071,-
0.815963,-0.142720,0.214080,-0.636606,-0.458295,0.515079,0.380445,0.365180,-0.407205,0.000000,0.000000
0,-0.174796,0.236674,0.21032,-0.529196,-0.163313,0.305531,0.112583,0,0.147328,-0.538023,0.685848,0.721758,-0.504234,-0.37368,-
0.56052,0.318265,-0.599959,0.674296,0.072672,-0.365180,0.203641,-0.525744,0.587803

RESTING STATE SCANS – SLICE TIMING

Resting state scans are labeled according to BIDS standard “task-rest”. Slice timing is included in the JSON when available. Some original DICOM files did not have slice timing info. [When slice timing information is unavailable use the ratio TR/#slices.](#)

ASL PARAMETERS

The following parameters are important for processing ASL images but were not extracted into the JSON files as part of the BIDS conversion.

Table 7. ASL Parameters by scanner

| Scanner model | Software Version | TI1 | TI2 | Labeling Strategy | Slice Readout | Background Suppression |
|---------------|------------------|-----|------|-------------------|---------------|------------------------|
| 51010 | syngo_MR_B18P | 700 | 1900 | PASL | 46.0ms | None |
| 51010 | syngo_MR_B20P | 700 | 1900 | PASL | 46.0ms | None |
| 35177 | syngo_MR_B17P | 700 | 1900 | PASL | 36.4ms | None |
| 35248 | syngo_MR_B17P | 700 | 1800 | PASL | 36.4ms | None |
| 175614 | | | | PASL | | |

POST-PROCESSED MRI: VOLUMETRIC SEGMENTATION

Single T1w MRI images were processed through Freesurfer to provide volumetric MRI data and segmentations maps. These maps can be used for a variety of purposes such as determining cortical volumes or regions of interest (ROIs) for PET imaging.

FREESURFER

OASIS-3 is a retrospective project that required anonymization of all files. In order to anonymize FreeSurfer output the following were removed: dates, timestamps, QC staff, raw file paths, original directory paths, ID change, and removal of all logs. OASIS-3 provides volumetric values representing Surface Measures from the aparc.stats Freesurfer output file and Subcortical Segmentation from the aseg.stats Freesurfer output file. These can be downloaded in csv format. All additional files, t1.mgz, brainmasks, segmentations, surface maps, and regional statistics.

**Conversion to BIDS format was completed following FreeSurfer processing. Segmentation of nifti files will produce different values than segmentation completed on dicom files and is documented by FreeSurfer. Direct comparison to OASIS-3 FreeSurfer files should be done using the T1.mgz file.*

For a full description of Subcortical Segmentation and Surface Measures statistical variable see [list](#).

PROCESSING BACKGROUND

FreeSurfer (<http://surfer.nmr.mgh.harvard.edu/>) analyses involved cortical reconstruction and volumetric segmentation of T1 weighted images.

The technical details of these procedures are described in prior publications (Dale et al., 1999; Dale and Sereno, 1993; Fischl and Dale, 2000; Fischl et al., 2001; Fischl et al., 2002; Fischl et al., 2004a; Fischl et al., 1999a; Fischl et al., 1999b; Fischl et al., 2004b; Han et al., 2006; Jovicich et al., 2006; Segonne et al., 2004)). The processing pipeline included motion correction and segmentation of the subcortical white matter and deep gray matter volumetric structures on a T1 weighted image (Fischl et al., 2002), intensity normalization, registration to a spherical atlas which utilized individual cortical folding patterns to match cortical geometry across subjects (Fischl et al., 1999b), and parcellation of the cerebral cortex into units based on gyral and sulcal structure (Desikan et al., 2006).

All MRI sessions were processed through the FreeSurfer image analysis suite using Dell PowerEdge 1950 servers with Intel Xeon processors running CentOS 5.5 Linux.

- All 1.5T imaging data was reprocessed using FreeSurfer 5.0 or FreeSurfer 5.1.
- All 3.0T MRI imaging data was reprocessed using FreeSurfer 5.3-HCP-patch.
- All data (1.5 and 3.0 T) have been corrected per the 2012 patch released by MGH.

QUALITY CONTROL MEASURES

Individuals responsible for processing imaging data are trained in the FreeSurfer quality control (QC) measures developed by the KARI Imaging Core. During the QC process, the rater will locate all FreeSurfer errors in the cortical parcellation and subcortical segmentation that meet a certain size based on the QC criteria below. An error that meets the QC criteria will require manual intervention (editing the FreeSurfer) and/or will fail quality control. There are two main types of FreeSurfer QC errors: inclusion and exclusion. Inclusion errors are identified as non-brain regions (dura, skull, etc.) that are being assessed as part of the brain and exclusion errors are identified as brain regions that are excluded from the cortical/subcortical classification. Generally, three attempts will be made to fix FreeSurfer QC errors if the error persists after performing edits. After the third attempt, the FreeSurfer will either pass with a note indicating that edits were performed or fail QC depending on the size of the error

OASIS-3 includes FreeSurfer output for sessions that were of quality “pass” or “pass with edits”.

FreeSurfer QC criteria is as follows:

- Dural inclusion, gray matter exclusion, sulcus inclusion, cerebellum inclusion will require edits if equal to or larger than 120 voxels (mm³).
- Cerebellum, subcortical and hippocampus segmentation exclusion will fail quality control if greater than 120 voxels (mm³). Before failing, other errors will be fixed if possible, which may fix segmentation exclusions.
- White matter exclusion will require edits if equal to or larger than 60 voxels (mm³).
- Lateral ventricle segmented incorrectly will require edits if equal to or larger than 300 voxels (mm³).

ANALYSIS CONSIDERATIONS

CORRECTING SUBCORTICAL AND CORTICAL VOLUMES FOR HEAD SIZE

It is suggested that all regions volumes should be corrected for head size (intracranial volume, ICV) in order to have correct comparisons. This does not apply to cortical thickness measures, as cortical thickness does not significantly vary with head size. The normalization process applies to each individual ROI and is sample specific. Please note if participants are removed from the data set the normalizations on the subcortical volumes will need to be re-run.

Note: Volume normalization must be repeated every time a subject is added or removed from the sample.

To test the consistency of FreeSurfer derived ICV, an analysis of the ICV estimate for each participant was performed on a longitudinal cohort (Figure 2). All participants had MRI scans using a 3T scanner and were processed with FreeSurfer 5.3. Within a participant, ICV can vary from baseline more than 5% with a mean subject standard deviation of 15.75 cm³. This variance should be taken into consideration when correcting subcortical and cortical volumes.

Relevant publication for the head-size correction:

Randy L. Buckner, Denise Head, Jamie Parker, Anthony F. Fotenos, Daniel Marcus, John C. Morris, and Abraham Z. Snyder A unified approach for morphometric and functional data analysis in young, old, and demented adults using automated atlas-based head size normalization: reliability and validation against manual measurement of total intracranial volume. *Neuroimage*, 2004.

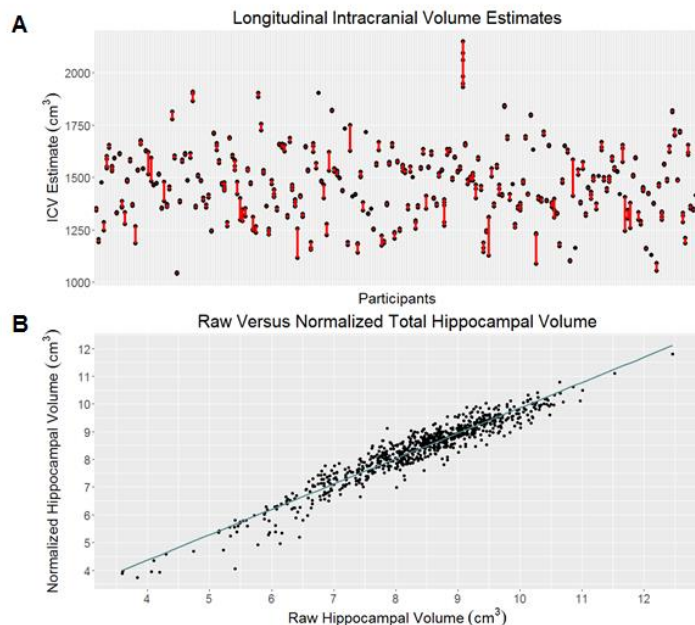


Figure 2 (A) ICV estimate for each participant in a longitudinal study. Each black circle represents an MR session and the red line represents a longitudinal participant. (B) The relationship between the raw hippocampal volume and the hippocampal volume normalized by ICV.

INSTRUCTIONS FOR NORMALIZATION OF MRI FREESURFER-DERIVED CORTICAL VOLUMES

Normalization Calculation:

1. Compute mean ICV for sample
2. Compute regression with ICV as independent variable and ROI as dependent variable to obtain B (NOT Beta) weight
3. Compute: **Normalized = raw volume – (B-weight * (ss ICV – mean ICV))**
[Note: "ss" = single subject's]
4. This procedure is repeated for each subcortical & cortical ROI volume the investigator is interested in.
 - a. These volumes can be found in the "aseg.stats" file.
 - b. We do not normalize the cortical thickness measures.

Table 8. Below shows a snapshot from the SPSS output for the linear regression. Use the B value highlighted in red for the correction factor. This will be repeated for each given ROI.

| Coefficients ^a | | | | | |
|---------------------------|------------|-----------------------------|------------|---------------------------|-------|
| Model | | Unstandardized Coefficients | | Standardized Coefficients | |
| | | B | Std. Error | Beta | |
| 1 | (Constant) | 2718.207 | 343.943 | | 7.903 |
| | ICV | -1.513E-5 | .000 | -.008 | .946 |

a. Dependent Variable: transtemp

ADDITIONAL REGIONAL CALCULATIONS

Regional FreeSurfer outputs can be combined to generate multiple global brain measures that researchers may find useful (see <https://surfer.nmr.mgh.harvard.edu/fswiki/MorphometryStats>):

- Whole Brain Volume = Cortex + CorticalWhiteMatter + SubCortGray
- Cortex = lhCortex + rhCortex
- CorticalWhiteMatter = lhCorticalWhiteMatterVol + rhCorticalWhiteMatterVol
- SubCortGray = summation of thalamus, caudate, hippocampus, amygdala, accumbens, ventral DC, substantia nigra (if there). This is a simple voxel count of structures identified as subcortical GM.
- Total Ventricular Volume = left and right lateral inferior lateral ventricles + 3rd + 4th + 5th ventricles)

MR SCANNER COMPERISON: SIEMENS TIM TRIO 3T AND SIEMENS BIOGRAPH 3T MMR

In order to combine data from both the Siemens TIM Trio 3T MRI and the Siemens Biograph 3T mMR (PET MR), a direct correlation was performed in a subset of our participants. For the scanner validation, 69 participants with a mean age of 65.9 years (CDR 0-0.5) received both the Trio and mMR MRI within two weeks. Of the 69 participants, 67 participants were CN (CDR 0) and 2 participants had a diagnosis of mild symptomatic AD (CDR 0.5). FreeSurfer v5.1 was used to segment the brain into various regions of interest (ROI) for quantitative analysis.

For the left hippocampal volume as measured by Trio and the PET MR, the estimated concordance correlation coefficient (CCC) on the raw data is 0.83 with a 95% CI from 0.73 to 0.89, and after the standardization, the estimated CCC is 0.83 with a 95% CI from 0.74 to 0.90. For the right hippocampus volume as measured by Trio and the PET MR, the estimated CCC on the raw data is 0.79 with a 95% CI from 0.67 to 0.87, and after the standardization, the estimated CCC is still 0.79 with a 95% CI from 0.67 to 0.87.

Because of the two potential outliers on the hippocampal volumes data (Figure 3), rank-based CCC was performed on these measures. The rank-based CCC for left hippocampal volume is 0.92 with a 95% CI from 0.86 to 0.95, and the rank-based CCC for right hippocampal volume is 0.91 with a 95% CI from 0.86 to 0.95; both indicating excellent rank-based reproducibility of measuring hippocampal volumes. These findings are within the reported test-retest reliability range for repeat MRI visits on the same scanner (Han et al., 2006).

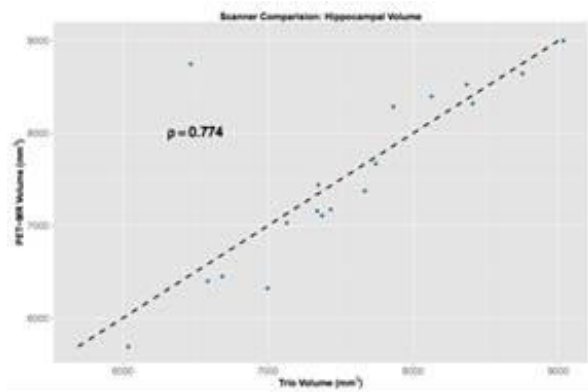


Figure 3. Hippocampal volume comparison of FreeSurfer derived hippocampal volumes from the Siemens TIM Trio 3T MRI and the Siemens Biograph mMR 3T PET-MR.

PET IMAGING

PET SCANNERS

Data included in OASIS was collected on the following scanners. Scanner specific information is recorded in dataset_description.json for each MR scan session. *For manuscripts, select only the scanner(s) from which your subset of data were derived.*

- Siemens Biograph mMR PET-MR 3T scanner (serial#: 51010)
- Siemens Biograph 40 PET/CT scanner (serial#: 1003)
- Siemens Biograph 128_Vision Edge PET/CT (serial#: 11009)
- Siemens ECAT HRplus 962 PET scanner (serial#: 101006)

HR+ IMAGE NOTES (PIB AND FDG)

ECAT PET images were acquired on either a Siemens 962 HR+ PET scanner. Emission data were reconstructed using a 3-D filter back-projection into a 128 x 128 x 63 matrix (2.12 x 2.12 x 2.43mm) with single scatter correction [1], a ramp filter (resolution of ~5.5-6 mm full-width half maximum [FWHM]), measured attenuation factors from a Ge-68 transmission scan, and randoms correction. These images have been converted from ECAT to NIFTI using dcm2niix (v1.0.20180404 GCC4.4.7).

All processed data have already been spatially smoothed to a FWHM of 8mm using the PET Unified Pipeline (PUP). To achieve a FWHM of 8mm for data harmonization of the ECAT images, we recommend the following Gaussian kernels to be in alignment with the Alzheimer's Disease Neuroimaging Initiative (ADNI) protocol FWHM all planes = 5.5 mm for the Siemens HR+.

TRACERS

PIB

N-methyl- $[^{11}\text{C}]2$ -(4'-methylaminophenyl)-6-hydroxybenzothiazole ($[^{11}\text{C}]\text{PIB}$) is a radiolabeled compound that binds *in vivo* to brain amyloid deposits. Developed at the University of Pittsburgh, PIB has very high affinity for amyloid plaques. With administration of 6 - 20 mCi of $[^{11}\text{C}]\text{PIB}$, a 60 minute dynamic PET scan in 3D mode (septa retracted) will be initiated (24 x 5 sec frames; 9 x 20 sec frames; 10 x 1 min frames; 9 x 5 min frames).

AV45

Florbetapir binds to β -amyloid ($\text{A}\beta$) plaque utilizing the radioactive isotope ^{18}F for use in PET scanning. Florbetapir ^{18}F is used under the research number ^{18}F -AV-45 and therefore referred to as AV45. Participants received a single i.v. administration of approximately 370 MBq (10 mCi) of florbetapir ^{18}F (over 10-60 sec). There are two acceptable procedures for obtaining the florbetapir ^{18}F PET scans:

1. In the preferred approach, the participant will be positioned in the PET-MR scanner at the time of injection and a 70-minute dynamic scan (with simultaneous PET and full Standard MR acquisition) will be

obtained starting at the time of injection. For florbetapir F 18 scans conducted on the PET/MR scanner, a short (approximately 15 minute) CT scan may be conducted on the PET/CT scanner.

2. For those participants who cannot tolerate the full exam, an alternative is to rest quietly in an uptake room for the first 40 minutes after injection. The participant will then be positioned in the PET-MR scanner to undergo a scan lasting 20 minutes, beginning 50 minutes after florbetapir F 18 injection and lasting for 20 minutes, using the Short MR Protocol. For florbetapir F 18 scans conducted on the PET/MR scanner, a short (approximately 15 minute) CT scan may be conducted on the PET/CT scanner.

FDG

Metabolic imaging with [18F]FDG-PET was performed with a 3D dynamic acquisition began 40 minutes after a bolus injection of approximately 5 mCi of FDG and lasted for 20 minutes.

AV1451

Flortaucipir binds to the paired helical filaments characteristic of neurofibrillary tau tangles in Alzheimer disease. Flortaucipir F18 is used under the research name 18F-AV-1451 and therefore referred to as AV1451. Participants received a single i.v. administration of approximately 370 MBq (10 mCi) of flortaucipir F18 (over 10-60 sec). There are three acceptable procedures for obtaining flortaucipir F18 PET scans:

1. In the preferred approach, the participant will be positioned in the PET/CT scanner at time of injection and a 105-minute dynamic scan will be acquired starting at time of injection.
2. For participants who cannot tolerate the full exam, an alternative is to rest quietly in an uptake room for the first 75-minutes after injection. The participant will then be positioned in the PET/CT to undergo a scan lasting 30 minutes.
3. A final alternative is a hybrid approach. In this method, the participant will be positioned in the PET/CT scanner at time of injection and a 60-minute dynamic scan will be acquired starting at time of injection. The participant will then have a 15-minute rest period where they are free to leave the scanner. Following this 15-minute break period, the participant will be placed back into the PET/CT and a 30-minute static scan will be acquired starting at 75-minutes post-injection. The two scans will be reconstructed separately from one another. This method accommodates participants who are unable to complete the full, uninterrupted exam while persevering early frame dynamic information.

POST-PROCESSED PET: PET UNIFIED PIPELINE (PUP)

PET imaging analyses are performed using the PET unified pipeline (PUP, <https://github.com/ysu001/PUP>) (Su 2013, Su 2015).

PET images are smoothed to achieve a common spatial resolution of 8mm to minimize inter-scanner differences (Joshi et al., 2009). Inter-frame motion correction for the dynamic PET images is performed using standard image registration techniques (Hajnal et al., 1995; Eisenstein et al., 2012). PET-MR registration is performed using a vector-gradient algorithm (VGM; Rowland et al., 2005) in a symmetric fashion (i.e. average transformation for PET-

>MR and inverse of MR->PET was used as the final transformation matrix). By default, regional PET processing is performed based on FreeSurfer segmentation (using wmparc.mgz as the region definition), and each FreeSurfer region is analyzed. The PET processing pipeline generates both reports of regional measurements as well as an SUVR image in the individual FreeSurfer space.

PUP VARIABLE NOMENCLATURE

Our data naming convention provides a standard for listing the region and the processing method (Table 8). Left and right brain structures use L and R. When left and right are averaged together the suffix includes the designation TOT. For a full list of variables see [PUP Variables](#). Six prefixes are used:

Table 9 PUP Nomenclature

| Data Type | Definition | Example Name |
|------------|---|-------------------------|
| fBP_ | <i>FreeSurfer calculated Binding Potential</i> | fBP_TOT_ACCUMBENS |
| fBP_rsf_ | <i>FreeSurfer calculated, partial volume corrected Binding Potential</i> | fBP_rsf_TOT_ACCUMBENS |
| fSUVR_ | <i>FreeSurfer calculated SUVR</i> | fSUVR_TOT_ACCUMBENS |
| fSUVR_rsf_ | <i>FreeSurfer calculated, partial volume corrected SUVR, the gold standard</i> | fSUVR_rsf_TOT_ACCUMBENS |
| ASL_ | <i>Arterial Spin Labeled Cerebral Blood Flow</i> | ASL_TOT_ACCUMBENS |
| ASL_pvc_ | <i>Arterial Spin Labeled Cerebral Blood Flow with Partial Volume Correction</i> | ASL_pvc_TOT_ACCUMBENS |

Table 10 PUP prefixes (tracer+processed_outcome) examples

| Tracer | Definition | Example Name |
|--------|-----------------------------------|--------------------------|
| FDG | <i>[18F]-Fluodeoxyglucose</i> | FDG_fSUVR_TOT_ACCUMBENS |
| PiB | <i>[11C]-Pittsburg Compound B</i> | PiB_fBP_TOT_ACCUMBENS |
| AV45 | <i>[18F]-Florbetapir</i> | AV45_fSUVR_TOT_ACCUMBENS |

The prefixes (tracer+processed_outcome) are applied to the SAS correlate suffix to create a descriptive SAS compliant name (Table 9).

- PiB_fSUVR_rsf_TOT_CTX_PRECUNEUS is the [11C] PiB partial volume corrected SUVR of the gray matter in both the right and left FreeSurfer precuneus.
- FDG_fSUVR_rsf_TOT_WM_PRECUNEUS is the [18F] FDG partial volume corrected SUVR of the white matter calculated using the average activity in both the right and left FreeSurfer precuneus.
- FDG_fBP_TOT_CORTMEAN is the [18F] FDG average BP of the four MCBP cortical structures using FreeSurfer regions (TOTFS_PREFRN, TOTFS_TMP, TOTFS_GYREC, TOT_CTX_PRECUNEUS).

PARTIAL VOLUME CORRECTION

As PET images have low spatial resolution, measured signals are distorted by partial volume effects (PVE). The distortion caused by PVE is a function of the size and shape of the region of interest in addition to spatial resolution of the images. In longitudinal studies, the impact of PVE is further confounded by brain atrophy due to aging and pathological changes. To account for these distortions, correction technique is implemented in our processing pipeline using a regional spread function (RSF; Rousset 1998) based approach (Su 2015). We have demonstrated that the RSF technique was able to improve PET quantification and achieve better sensitivity to

longitudinal changes in amyloid burden (Su 2015, 2016). Our standard PET processing includes results both with and without RSF partial volume correction. Also, SUVR images are only available without partial volume correction in current analysis.

ALTERNATIVE REFERENCE REGION

As previously described, cerebellum cortex is used as the standard reference region for image quantification. However, for SUVR measurements, it is possible to renormalize to any alternative reference region by dividing the standard SUVR value by the SUVR value of the alternative reference region of choice:

$$\text{SUVR}_{\text{new}} = \text{SUVR}_{\text{std}} / \text{SUVR}_{\text{altref}}$$

AMYLOID PET IMAGING ANALYSIS

Currently, two amyloid imaging tracers are used in our studies, i.e. [11C]-Pittsburgh Compound B (PiB) and [18F]-Florbetapir (AV45). For both tracers, two modeling approaches are implemented: 1) binding potential (BPND) is calculated using Logan graphical analysis (Logan 1996; Mintun 2006; Su 2013, 2015, 2016), when full dynamic PET imaging data are available, i.e. PET acquisition was started in synchronization with tracer administration and PET images were reconstructed into multiple time frames; 2) regional target-to-reference intensity ratio, a.k.a, standard uptake ratio (SUVR), is estimated for all processable PET data.

Under standard protocol, quantitative PET analysis (both BP_{ND} and SUVR) uses 30 to 60 minutes post-injection as the time window for PiB, and 50 to 70 minutes for AV45; and the cerebellum cortex is used as the default reference region. To assess global amyloid burden based on amyloid PET imaging data, the arithmetic mean of BPND or SUVRs from precuneus (PREC), prefrontal cortex (PREF), gyrus rectus (GR), and lateral temporal (TEMP) regions are defined as the mean cortical binding potential (MCBP) or mean cortical SUVR (MCSUVR). In FreeSurfer based processing, PREC is defined as the combined left and right hemisphere ctx-precuneus, PREF is defined as the left and right combined ctx-superiorfrontal and ctx-rostralmiddlefrontal regions, GR is defined as the left and right combined ctx-lateralorbitofrontal and ctx-medialorbitofrontal regions, and TEMP is defined as the left and right combined ctx-superialtemporal and ctx-middletemporal regions (Fig. 4; Su 2013).

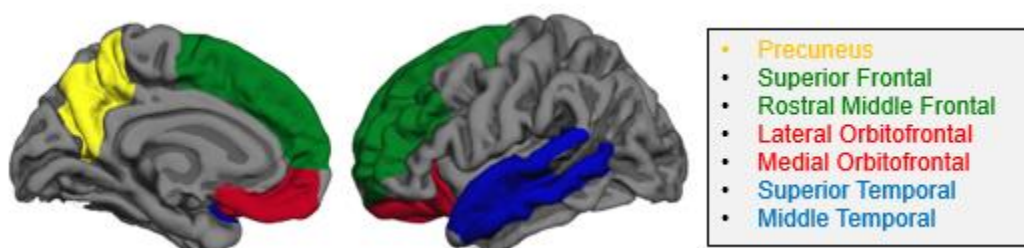


Figure 4 FreeSurfer regions for global amyloid burden index (MCBP, MCSUVR, etc) calculation.

CUTOFF VALUES FOR AMYLOID POSITIVITY

Traditionally, the cutoff for amyloid positivity has been established as MCBP>0.18 based on manually processed PiB data (Mintun 2006). We also established that the same cutoff could be used for FreeSurfer processing generated MCBP based on a study population of 77 participants (Su 2013). Based on this dataset, the cutoff for MCSUVR_{RSF} was determined to be 1.42, the cutoff values for additional versions of global amyloid burden measurements that would generate best matched amyloid positivity classification as using manual MCBP=0.18 are also determined. For AV45, the equivalent cutoff to PiB MCSUVR_{RSF}>1.42 was determined based on a sporadic AD cohort of 103 participants who had AV45-PiB crossover data based on the regression line between AV45 MCSUVRs and PiB MCSUVR_{RSF} (Fig. 5) (Su 2019). The amyloid positivity cutoff using the cerebellar cortex reference region (Table 11), brainstem reference region (Table 12), and centiloid values (Table 13) are found below.

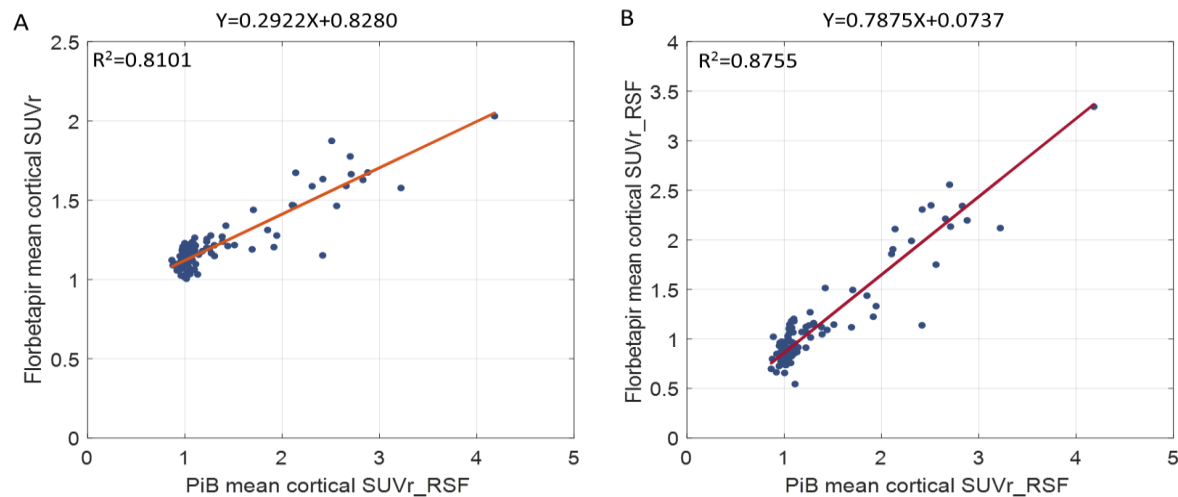


Figure 5. PiB-AV45 crossover dataset illustrating the relationship between AV45 based mean cortical SUVR and PiB based mean cortical SUVRs.

Table 11. Amyloid Positivity Cutoffs - Cerebellar Cortex Reference Region (*see Su et al 2019)

| Amyloid Positivity Cutoffs - Cerebellar Cortex Reference Region | |
|---|--------|
| PIB MCBP | 0.18 |
| PIB MCBP RSF | 0.37 |
| PIB MCSUVR | 1.31 |
| PIB MCUSVR RSF | 1.42 |
| AV45 MCSUVR | 1.24 * |
| AV45 MCSUVR RSF | 1.19 * |

Table 12. Amyloid Positivity Cutoffs – Brainstem Reference Region

| Amyloid Positivity Cutoffs – Brainstem Reference Region | |
|---|------|
| PIB MCSUVR BS | 0.79 |
| PIB MCUSVR RSF BS | 0.72 |

Table 13. The equivalent cutoffs in Centiloid units were also derived by applying the Centiloid conversion equations described below to the native measurement cutoffs.

| Amyloid Positivity Cutoffs - Centiloid | |
|--|------|
| CL PIB MCBP | 18.2 |
| CL PIB MCUSVR RSF | 16.4 |
| CL AV45 MCSUVR | 21.9 |
| CL AV45 MCSUVR RSF | 20.6 |

CENTILOID CONVERSION FOR AMYLOID PET

Differences in the amyloid imaging tracer, the PET acquisition, and the analysis protocol across different studies introduce considerable variability within amyloid PET imaging data. This variability leads to difficulties in comparing and interpreting amyloid burden results reported from different groups (Klunk et al, 2015). To achieve comparable results, the Centiloid Working Group established a standardized scale called Centiloid to convert mean cortical SUVR and BP into a Centiloid measure of global amyloid disposition. If you want to use regional values, consult the Imaging Core.

The procedure and requirements to define the Centiloid scale is documented in detail in the initial Centiloid paper (Klunk et al 2015). To summarize, the Centiloid scale is defined by two anchor points: the mean amyloid burden measurement of a young control group with no amyloid pathology in their brain, represented as 0 in the Centiloid scale, and the mean amyloid burden of an AD group, represented as 100 in the Centiloid scale (level 1 calibration). Subsequently, a Deming regression and a linear transformation are performed to calibrate the tracer and the local processing methods to the Centiloid scale (i.e. level 2 calibration). Currently, both PiB and AV45 have been calibrated to the Centiloid scale for both non-partial volume and partial volume correction (rsf) using standard PUP (see equations below).

The PiB-Centiloid equations were defined using a subset of the Global Alzheimer’s Association Information Network dataset (GAAIN, <http://www.gaain.org>) for PiB (30-60 minutes post-injection) SUVR and BP measures and were processed with cerebellar cortex, whole cerebellum, or brainstem as the reference region. Different reference regions have an impact on the mean Centiloid values and we suggest using the cerebellar cortex as the reference region since it has the least variability in the young control cohort (eq. 1 through 4). We found that our implementation of the standard Centiloid analysis is strongly correlated with the published Centiloid measures for the GAAIN data set ($r^2 = 0.99$).

The AV45-Centiloid equations (eq.5 and 6) were defined using a subset of the baseline DIAN trial unit (DIAN-TU) data set with PiB (40-70 minutes post-injection) and AV45 (50-70 minutes post-injection) imaging data for SUVR measures; the cerebellar cortex was used as the default reference region. A strong correlation ($r^2 = 0.79$) was found, shown in figure 6, between AV45 mean cortical SUVRs and PiB Centiloid SUVRs (SUVRs calculated through the Centiloid pipeline) (Klunk et al. 2015).

As any tracer or processing method can be scaled to Centiloid, new equations will be derived as new amyloid tracers and data become available. Centiloid equations may be recalibrated in the future to follow consensus of the research community.

Table 14. Centiloid conversion equations for PiB and AV45 using the "tot_cortmean" variable.

| Centiloid Equations (TOT_CORTMEAN) | | |
|---|--|------|
| $\text{PiB}_{\text{Centiloid}_{\text{BP}}} = 126.7 \times \text{PiB_3060_BP} - 4.4$ | | Eq.1 |
| $\text{PiB}_{\text{Centiloid}_{\text{SUVR}}} = 111.8 \times \text{PiB_3060_SUVR} - 119.3$ | | Eq.2 |
| $\text{PiB}_{\text{Centiloid}_{\text{BPRS}}} = 53.9 \times \text{PiB_3060_BP_RSF} - 4.7$ | | Eq.3 |
| $\text{PiB}_{\text{Centiloid}_{\text{SUVR}_{\text{RSF}}}} = 45.0 \times \text{PiB_3060_SUVR_RSF} - 47.5$ | | Eq.4 |
| $\text{AV45}_{\text{Centiloid}_{\text{SUVR}}} = 163.6 \times \text{AV45_SUVR} - 181.0$ | | Eq.5 |
| $\text{AV45}_{\text{Centiloid}_{\text{SUVR}_{\text{RSF}}}} = 53.6 \times \text{AV45_SUVR_RSF} - 43.2$ | | Eq.6 |

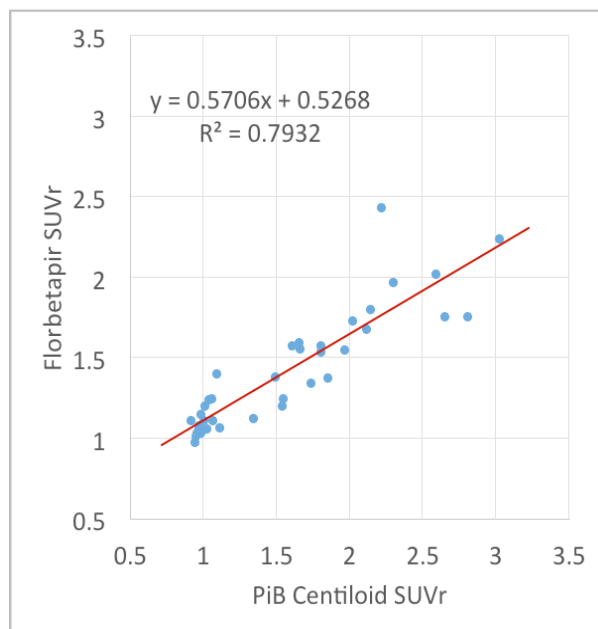


Figure 6 Comparison between PiB Centiloid SUVR and AV45 mean cortical SUVR for the DIAN-TU calibration dataset.

Table 15 below shows some examples on the conversion of non-partial volume corrected SUVR and BP to their respective Centiloid value.

| Centiloid Value | PiB 30-60 min BP | PiB 30-60 min SUVR |
|-----------------|------------------|--------------------|
| -10 | -0.0442 | 0.9776 |

| | | |
|-----|--------|--------|
| 0 | 0.0347 | 1.0671 |
| 25 | 0.2320 | 1.2907 |
| 50 | 0.4294 | 1.5143 |
| 75 | 0.6267 | 1.7379 |
| 100 | 0.8240 | 1.9615 |
| 110 | 0.9029 | 2.0510 |

ADRC conversion equations additionally have been defined between PiB (30-60 minutes post-injection) and AV45 (50-70 minutes post-injection) using the same DIAN-TU Centiloid calibration cohort (mentioned above) for the non-partial volume and partial volume corrected MCSUVRs measures (eq. 7 through 10).

Table 16 Conversion Equations between PiB and AV45 (TOT_CORTMEAN).

| Conversion Equations between PiB and AV45 (TOT_CORTMEAN) | | |
|--|--|-------|
| PIB MCSUVR | $= (AV45_MCSUVR - 0.3678) / 0.6942$ | Eq.7 |
| AV45 MCSUVR | $= (PiB_3060_MCSUVR * 0.6942) + 0.3678$ | Eq.8 |
| PIB MCSUVR_{RSF} | $= (AV45_MCSUVR_RSF - 0.0238) / 0.7948$ | Eq.9 |
| AV45 MCSUVR_{RSF} | $= (PiB_3060_MCSUVR_RSF * 0.7948) + 0.0238$ | Eq.10 |

TAU PET IMAGING (OASIS3_AV1451)

[18F]-Flortaucipir (AV-1451) previously known as T807 (Chien 2013) is currently used for in vivo imaging of tau pathology in Knight ADRC studies. Standard procedure for tau PET processing is identical to amyloid PET processing with the exception of the time window (80-100 minutes) that used for quantification.

Tau PET data is accessible in a separate protected project on central.xnat.org and linked to OASIS-3 subjects. Access can be granted by emailing the following information to oasis-brains@nrg.wustl.edu:

- 1 page summary of research proposal
- List of investigators to add (names and emails)
- Signed data use agreement (digital signature accepted)

BRAAK STAGING

The progression of Alzheimer disease related neurofibrillary pathology can be determined by Braak staging (Braak and Braak 1995). The six stages are calculated for the AV1451 tracer and included in the OASIS3_AV1451 sub-project releases (Table 17).

Table 17. The regions included in each Braak staging measure.

| Braak Stage | FS Region Processing Name | Biostatistics Standardizations |
|-------------|------------------------------|--------------------------------|
| 1-2 | ctx-entorhinal | fSUVR_rsf_TOT_CTX_ENTORHINAL |
| 3-4 | Amygdala | fSUVR_rsf_TOT_AMYGDALA |
| 3-4 | Accumbens-area | fSUVR_rsf_TOT_ACCUMBENS |
| 3-4 | hippocampus | fSUVR_rsf_TOT_HIPPOCAMPUS |
| 3-4 | ctx-insula | fSUVR_rsf_TOT_CTX_INSULA |
| 3-4 | ctx-medialorbitofrontal | fSUVR_rsf_TOT_CTX_MEDORBFRN |
| 3-4 | ctx-lateralorbitofrontal | fSUVR_rsf_TOT_CTX_LATORBFRN |
| 3-4 | ctx-parsorbitalis | fSUVR_rsf_TOT_CTX_PARSORBLS |
| 3-4 | ctx-parahippocampal | fSUVR_rsf_TOT_CTX_PARAHPCMPL |
| 3-4 | ctx-rostralanteriorcingulate | fSUVR_rsf_TOT_CTX_ROSANTCNG |
| 3-4 | ctx-posteriorcingulate | fSUVR_rsf_TOT_CTX_POSTCNG |
| 3-4 | ctx-caudalanteriorcingulate | fSUVR_rsf_TOT_CTX_CAUDANTCNG |
| 3-4 | ctx-isthmuscingulate | fSUVR_rsf_TOT_CTX_ISTHMUSCNG |
| 5-6 | ctx-bankssts | fSUVR_rsf_TOT_CTX_SSTSBANK |
| 5-6 | ctx-middletemporal | fSUVR_rsf_TOT_CTX_MIDTMP |
| 5-6 | ctx-caudalmiddlefrontal | fSUVR_rsf_TOT_CTX_CAUDMIDFRN |
| 5-6 | ctx-fusiform | fSUVR_rsf_TOT_CTX_FUSIFORM |
| 5-6 | ctx-inferiorparietal | fSUVR_rsf_TOT_CTX_INFERPRTL |
| 5-6 | ctx-inferiortemporal | fSUVR_rsf_TOT_CTX_INFERTMP |
| 5-6 | ctx-lateraloccipital | fSUVR_rsf_TOT_CTX_LATOCC |
| 5-6 | ctx-supramarginal | fSUVR_rsf_TOT_CTX_SUPRAMRGNL |
| 5-6 | ctx-precuneus | fSUVR_rsf_TOT_CTX_PRECUNEUS |

CUTOFF VALUES FOR TAU POSITIVITY

A tau summary measure, labeled as ‘tauopathy’, has been defined by our group to be the arithmetic mean of the partial volume corrected SUVRs from the amygdala, entorhinal cortex, inferior temporal region, and lateral occipital cortex defined using Freesurfer. (Mishra et al., 2017). Tables 18 specifies the tau positivity cutoff using the tauopathy measure.

Table 18. Tau positivity cutoff - Cerebellar Cortex Reference Region

| Tau Positivity Cutoff - Cerebellar Cortex Reference Region | |
|--|------|
| AV-1451 Tauopathy | 1.22 |

FREESURFER VARIABLES

Below is a list of the Freesurfer variables as found in OASIS-3 and a suggested list of SAS compatible labels.

| MRI Freesurfer Default Variable | SAS Compatible Variable Labels |
|---------------------------------------|--------------------------------|
| 3rd-Ventricle | MR_TOTV_THIRDVENT |
| 4th-Ventricle | MR_TOTV_FOURTHVENT |
| 5th-Ventricle | MR_TOTV_FIFTHVENT |
| Brain-Stem | MR_TOTV_BRAINSTEM |
| CC_Anterior | MR_TOTV_CRPCLM_ANT |
| CC_Central | MR_TOTV_CRPCLM_CNTRL |
| CC_Mid_Anterior | MR_TOTV_CRPCLM_MID_ANT |
| CC_Mid_Posterior | MR_TOTV_CRPCLM_MID_POST |
| CC_Posterior | MR_TOTV_CRPCLM_POST |
| CortexVol | MR_TOTV_CORTEX |
| CSF | MR_TOTV_CSF |
| IntraCranialVol | MR_TOTV_INTRACRANIAL |
| non-WM-hypointensities | MR_TOTV_NONWMHYPOINTENSITIES |
| Optic-Chiasm | MR_TOTV_OPTICHIASM |
| SubCortGrayVol | MR_TOTV_SUBCORTGRAY |
| TotalGrayVol | MR_TOTV_GRAY |
| WM-hypointensities | MR_TOTV_WMHYPOINTENSITIES |
| lh_bankssts_thickness | MR_LT_SSTSBANK |
| lh_caudalanteriorcingulate_thickness | MR_LT_CAUDANTCNG |
| lh_caudalmiddlefrontal_thickness | MR_LT_CAUDMIDFRN |
| lh_cuneus_thickness | MR_LT_CUNEUS |
| lh_entorhinal_thickness | MR_LT_ENTORHINAL |
| lh_frontalpole_thickness | MR_LT_FRNPOLE |
| lh_fusiform_thickness | MR_LT_FUSIFORM |
| lh_inferioparietal_thickness | MR_LT_INFRPRTL |
| lh_inferiortemporal_thickness | MR_LT_INFRTMP |
| lh_insula_thickness | MR_LT_INSULA |
| lh_isthmuscingulate_thickness | MR_LT_ISTHMUSCNG |
| lh_lateraloccipital_thickness | MR_LT_LATOCC |
| lh_lateralorbitofrontal_thickness | MR_LT_LATORBFRN |
| lh_lingual_thickness | MR_LT_LINGUAL |
| lh_medialorbitofrontal_thickness | MR_LT_MEDORBFRN |
| lh_middletemporal_thickness | MR_LT_MIDTMP |
| lh_paracentral_thickness | MR_LT_PARACNTRL |
| lh_parahippocampal_thickness | MR_LT_PARAHPCMPL |
| lh_parsopercularis_thickness | MR_LT_PARAOPRCLRS |
| lh_parsorbitalis_thickness | MR_LT_PARSORBLS |
| lh_parstriangularis_thickness | MR_LT_PARSTRNGLRS |
| lh_pericalcarine_thickness | MR_LT_PERICLCRN |
| lh_postcentral_thickness | MR_LT_POSTCNTRL |
| lh_posteriorcingulate_thickness | MR_LT_POSTCNG |
| lh_precentral_thickness | MR_LT_PRECNTRL |
| lh_precuneus_thickness | MR_LT_PRECUNEUS |
| lh_rostralanteriorcingulate_thickness | MR_LT_ROSANTCNG |
| lh_rostralmiddlefrontal_thickness | MR_LT_ROSMIDFRN |
| lh_superiorfrontal_thickness | MR_LT_SUPERFRN |
| lh_superioparietal_thickness | MR_LT_SUPERPRTL |
| lh_superiortemporal_thickness | MR_LT_SUPERTMP |
| lh_supramarginal_thickness | MR_LT_SUPRAMRGNL |
| lh_temporalpole_thickness | MR_LT_TMPPOLE |
| lh_transversetemporal_thickness | MR_LT_TRANSTMP |
| rh_bankssts_thickness | MR_RT_SSTSBANK |
| rh_caudalanteriorcingulate_thickness | MR_RT_CAUDANTCNG |
| rh_caudalmiddlefrontal_thickness | MR_RT_CAUDMIDFRN |

| | |
|---------------------------------------|----------------------------|
| rh_cuneus_thickness | MR_RT_CUNEUS |
| rh_entorhinal_thickness | MR_RT_ENTORHINAL |
| rh_frontalpole_thickness | MR_RT_FRNPOLE |
| rh_fusiform_thickness | MR_RT_FUSIFORM |
| rh_inferioparietal_thickness | MR_RT_INFRPRTL |
| rh_inferiortemporal_thickness | MR_RT_INFRTMP |
| rh_insula_thickness | MR_RT_INSULA |
| rh_isthmuscingulate_thickness | MR_RT_ISTHMUSCNG |
| rh_lateraloccipital_thickness | MR_RT_LATOCC |
| rh_lateralorbitofrontal_thickness | MR_RT_LATORBFRN |
| rh_lingual_thickness | MR_RT_LINGUAL |
| rh_medialorbitofrontal_thickness | MR_RT_MEDORBFRN |
| rh_middletemporal_thickness | MR_RT_MIDTMP |
| rh_paracentral_thickness | MR_RT_PARACNTRL |
| rh parahippocampal_thickness | MR_RT_PARAHPCMPL |
| rh_parsopercularis_thickness | MR_RT_PARAOPRCLRS |
| rh_parsorbitalis_thickness | MR_RT_PARSORBLS |
| rh_parstriangularis_thickness | MR_RT_PARSTRNGLRS |
| rh_pericalcarine_thickness | MR_RT_PERICLCRN |
| rh_postcentral_thickness | MR_RT_POSTCNTRL |
| rh_posteriorcingulate_thickness | MR_RT_POSTCNG |
| rh_precentral_thickness | MR_RT_PRECNTRL |
| rh_precuneus_thickness | MR_RT_PRECUNEUS |
| rh_rostralanteriorcingulate_thickness | MR_RT_ROSANTCNG |
| rh_rostralmiddlefrontal_thickness | MR_RT_ROSMIDFRN |
| rh_superiorfrontal_thickness | MR_RT_SUPERFRN |
| rh_superioparietal_thickness | MR_RT_SUPERPRTL |
| rh_superiortemporal_thickness | MR_RT_SUPERTMP |
| rh_supramarginal_thickness | MR_RT_SUPRAMRGNL |
| rh_temporalpole_thickness | MR_RT_TMPPOLE |
| rh_transversetemporal_thickness | MR_RT_TRANSTMP |
| Left-Accumbens-area | MR_LV_ACCUMBENS |
| Left-Amygdala | MR_LV_AMYGDALA |
| Left-Caudate | MR_LV_CAUD |
| Left-Cerebellum-Cortex | MR_LV_CBLL_CORTEX |
| Left-Cerebellum-White-Matter | MR_LV_CBLL_WM |
| Left-choroid-plexus | MR_LV_CHORPLEX |
| Left-Hippocampus | MR_LV_HIPPOCAMPUS |
| Left-Inf-Lat-Vent | MR_LV_INFLATVENT |
| Left-Lateral-Ventricle | MR_LV_LATVENT |
| Left-non-WM-hypointensities | MR_LV_NONWMHYPOINTENSITIES |
| Left-Pallidum | MR_LV_PALLIDUM |
| Left-Putamen | MR_LV_PUTAMEN |
| Left-Thalamus-Proper | MR_LV_THALAMUS |
| Left-VentralDC | MR_LV_VENTRALDC |
| Left-vessel | MR_LV_VESSEL |
| Left-WM-hypointensities | MR_LV_WMHYPOINTENSITIES |
| lh_bankssts_volume | MR_LV_SSTSBANK |
| lh_caudalanteriorcingulate_volume | MR_LV_CAUDANTCNG |
| lh_caudalmiddlefrontal_volume | MR_LV_CAUDMIDFRN |
| lh_cuneus_volume | MR_LV_CUNEUS |
| lh_entorhinal_volume | MR_LV_ENTORHINAL |
| lh_frontalpole_volume | MR_LV_FRNPOLE |
| lh_fusiform_volume | MR_LV_FUSIFORM |
| lh_inferioparietal_volume | MR_LV_INFRPRTL |
| lh_inferiortemporal_volume | MR_LV_INFRTMP |
| lh_insula_volume | MR_LV_INSULA |
| lh_isthmuscingulate_volume | MR_LV_ISTHMUSCNG |
| lh_lateraloccipital_volume | MR_LV_LATOCC |
| lh_lateralorbitofrontal_volume | MR_LV_LATORBFRN |
| lh_lingual_volume | MR_LV_LINGUAL |
| lh_medialorbitofrontal_volume | MR_LV_MEDORBFRN |
| lh_middletemporal_volume | MR_LV_MIDTMP |

| | |
|------------------------------------|-------------------|
| lh_paracentral_volume | MR_LV_PARACNTRL |
| lh_parahippocampal_volume | MR_LV_PARAHPCMPL |
| lh_parsopercularis_volume | MR_LV_PARAOPRCLRS |
| lh_parsorbitalis_volume | MR_LV_PARSORBLS |
| lh_parstriangularis_volume | MR_LV_PARSTRNGLRS |
| lh_pericalcarine_volume | MR_LV_PERICLCRN |
| lh_postcentral_volume | MR_LV_POSTCNTRL |
| lh_posteriorcingulate_volume | MR_LV_POSTCNG |
| lh_precentral_volume | MR_LV_PRECNTRL |
| lh_precuneus_volume | MR_LV_PRECUNEUS |
| lh_rostralanteriorcingulate_volume | MR_LV_ROSANTCNG |
| lh_rostralmiddlefrontal_volume | MR_LV_ROSMIDFRN |
| lh_superiorfrontal_volume | MR_LV_SUPERFRN |
| lh_superiorparietal_volume | MR_LV_SUPERPRTL |
| lh_superiortemporal_volume | MR_LV_SUPERTMP |
| lh_supramarginal_volume | MR_LV_SUPRAMRGNL |
| lh_temporalpole_volume | MR_LV_TMPPOLE |
| lh_transversetemporal_volume | MR_LV_TRANSTMP |
| lhCortexVol | MR_LV_CORTEX |
| lhCorticalWhiteMatterVol | MR_LV_CORTICALWMM |
| rh_bankssts_volume | MR_RV_SSTSBANK |
| rh_caudalanteriorcingulate_volume | MR_RV_CAUDANTCNG |
| rh_caudalmiddlefrontal_volume | MR_RV_CAUDMIDFRN |
| rh_cuneus_volume | MR_RV_CUNEUS |
| rh_entorhinal_volume | MR_RV_ENTORHINAL |
| rh_frontalpole_volume | MR_RV_FRNPOLE |
| rh_fusiform_volume | MR_RV_FUSIFORM |
| rh_inferiorparietal_volume | MR_RV_INFRPRTL |
| rh_inferiortemporal_volume | MR_RV_INFRTMP |
| rh_insula_volume | MR_RV_INSULA |
| rh_isthmuscingulate_volume | MR_RV_ISTHMUSCNG |
| rh_lateraloccipital_volume | MR_RV_LATOCC |
| rh_lateralorbitofrontal_volume | MR_RV_LATORBFRN |
| rh_lingual_volume | MR_RV_LINGUAL |
| rh_medialorbitofrontal_volume | MR_RV_MEDORBFRN |
| rh_middletemporal_volume | MR_RV_MIDTMP |
| rh_paracentral_volume | MR_RV_PARACNTRL |
| rh_parahippocampal_volume | MR_RV_PARAHPCMPL |
| rh_parsopercularis_volume | MR_RV_PARAOPRCLRS |
| rh_parsorbitalis_volume | MR_RV_PARSORBLS |
| rh_parstriangularis_volume | MR_RV_PARSTRNGLRS |
| rh_pericalcarine_volume | MR_RV_PERICLCRN |
| rh_postcentral_volume | MR_RV_POSTCNTRL |
| rh_posteriorcingulate_volume | MR_RV_POSTCNG |
| rh_precentral_volume | MR_RV_PRECNTRL |
| rh_precuneus_volume | MR_RV_PRECUNEUS |
| rh_rostralanteriorcingulate_volume | MR_RV_ROSANTCNG |
| rh_rostralmiddlefrontal_volume | MR_RV_ROSMIDFRN |
| rh_superiorfrontal_volume | MR_RV_SUPERFRN |
| rh_superiorparietal_volume | MR_RV_SUPERPRTL |
| rh_superiortemporal_volume | MR_RV_SUPERTMP |
| rh_supramarginal_volume | MR_RV_SUPRAMRGNL |
| rh_temporalpole_volume | MR_RV_TMPPOLE |
| rh_transversetemporal_volume | MR_RV_TRANSTMP |
| rhCortexVol | MR_RV_CORTEX |
| rhCorticalWhiteMatterVol | MR_RV_CORTICALWMM |
| Right-Accumbens-area | MR_RV_ACCUMBENS |
| Right-Amygdala | MR_RV_AMYGDALA |
| Right-Caudate | MR_RV_CAUD |
| Right-Cerebellum-Cortex | MR_RV_CBLL_CORTEX |
| Right-Cerebellum-White-Matter | MR_RV_CBLL_WM |
| Right-choroid-plexus | MR_RV_CHORPLEX |
| Right-Hippocampus | MR_RV_HIPPOCAMPUS |

| | |
|------------------------------|----------------------------|
| Right-Inf-Lat-Vent | MR_RV_INFLATVENT |
| Right-Lateral-Ventricle | MR_RV_LATVENT |
| Right-non-WM-hypointensities | MR_RV_NONWMHYPOINTENSITIES |
| Right-Pallidum | MR_RV_PALLIDUM |
| Right-Putamen | MR_RV_PUTAMEN |
| Right-Thalamus-Proper | MR_RV_THALAMUS |
| Right-VentralDC | MR_RV_VENTRALDC |
| Right-vessel | MR_RV_VESSEL |
| Right-WM-hypointensities | MR_RV_WMHYPOINTENSITIES |

PUP VARIABLES

Below is a list of the Pet Unified Pipeline (PUP) variables as found in OASIS-3 and a suggested list of SAS compatible labels. The prefixes (tracer+processed_outcome) are applied to the SAS correlate suffix to create a descriptive SAS compliant name (ex: PiB_mSUVR_TOT_ACCUMBENS).

| Structure Name | SAS Compatible Variable Labels |
|--------------------------------|--------------------------------|
| Accumbens_area | TOT_ACCUMBENS |
| Amygdala | TOT_AMYGDALA |
| Brain_Stem | TOT_BRAINSTEM |
| Caudate | TOT_CAUD |
| CC_Anterior | CRPCLM_ANT |
| CC_Central | CRPCLM_CNTRL |
| CC_Mid_Anterior | CRPCLM_MID_ANT |
| CC_Mid_Posterior | CRPCLM_MID_POST |
| CC_Posterior | CRPCLM_POST |
| Cerebellum_Cortex | TOT_CBLL_CORTEX |
| Cerebellum_White_Matter | TOT_CBLL_WM |
| choroid_plexus | TOT_CHORPLEX |
| ctx_bankssts | TOT_CTX_SSTSBANK |
| ctx_caudalanteriorcingulate | TOT_CTX_CAUDANTCNG |
| ctx_caudalmiddlefrontal | TOT_CTX_CAUDMIDFRN |
| ctx_corpuscallosum | TOT_CTX_CRPCLM |
| ctx_cuneus | TOT_CTX_CUNEUS |
| ctx_entorhinal | TOT_CTX_ENTORHINAL |
| ctx_frontalpole | TOT_CTX_FRNPOLE |
| ctx_fusiform | TOT_CTX_FUSIFORM |
| ctx_inferiorparietal | TOT_CTX_INFRPRTL |
| ctx_inferiortemporal | TOT_CTX_INFRTMP |
| ctx_insula | TOT_CTX_INSULA |
| ctx_isthmuscingulate | TOT_CTX_ISTHMUSCNG |
| ctx_lateraloccipital | TOT_CTX_LATOCC |
| ctx_lateralorbitofrontal | TOT_CTX_LATORBFRN |
| ctx_lh_bankssts | L_CTX_SSTSBANK |
| ctx_lh_caudalanteriorcingulate | L_CTX_CAUDANTCNG |
| ctx_lh_caudalmiddlefrontal | L_CTX_CAUDMIDFRN |
| ctx_lh_corpuscallosum | L_CTX_CRPCLM |
| ctx_lh_cuneus | L_CTX_CUNEUS |
| ctx_lh_entorhinal | L_CTX_ENTORHINAL |
| ctx_lh_frontalpole | L_CTX_FRNPOLE |
| ctx_lh_fusiform | L_CTX_FUSIFORM |
| ctx_lh_inferiorparietal | L_CTX_INFRPRTL |
| ctx_lh_inferiortemporal | L_CTX_INFRTMP |
| ctx_lh_insula | L_CTX_INSULA |
| ctx_lh_isthmuscingulate | L_CTX_ISTHMUSCNG |
| ctx_lh_lateraloccipital | L_CTX_LATOCC |
| ctx_lh_lateralorbitofrontal | L_CTX_LATORBFRN |
| ctx_lh_lingual | L_CTX_LINGUAL |
| ctx_lh_medialorbitofrontal | L_CTX_MEDORBFRN |
| ctx_lh_middletemporal | L_CTX_MIDTMP |

| | |
|---------------------------------|--------------------|
| ctx_lh_paracentral | L_CTX_PARACNTRL |
| ctx_lh parahippocampal | L_CTX_PARAHPCMPL |
| ctx_lh_parsopercularis | L_CTX_PARSOPRCLRS |
| ctx_lh_parsorbitalis | L_CTX_PARSORBLS |
| ctx_lh_parstriangularis | L_CTX_PARSTRNGLRS |
| ctx_lh_pericalcarine | L_CTX_PERICLCRN |
| ctx_lh_postcentral | L_CTX_POSTCNTRL |
| ctx_lh_posteriorcingulate | L_CTX_POSTCNG |
| ctx_lh_precentral | L_CTX_PRECNTRL |
| ctx_lh_precuneus | L_CTX_PRECUNEUS |
| ctx_lh_rostralanteriorcingulate | L_CTX_ROSANTCNG |
| ctx_lh_rostralmiddlefrontal | L_CTX_ROSMIDFRN |
| ctx_lh_superiorfrontal | L_CTX_SUPERFRN |
| ctx_lh_superiorparietal | L_CTX_SUPERPRTL |
| ctx_lh_superiortemporal | L_CTX_SUPERTMP |
| ctx_lh_supramarginal | L_CTX_SUPRAMRGNL |
| ctx_lh_temporalpole | L_CTX_TMPPOLE |
| ctx_lh_transversetemporal | L_CTX_TRANSTMP |
| ctx_lingual | TOT_CTX_LINGUAL |
| ctx_medialorbitofrontal | TOT_CTX_MEDORBFRN |
| ctx_middletemporal | TOT_CTX_MIDTMP |
| ctx_paracentral | TOT_CTX_PARACNTRL |
| ctx parahippocampal | TOT_CTX_PARAHPCMPL |
| ctx_parsopercularis | TOT_CTX_PARSOPCLRS |
| ctx_parsorbitalis | TOT_CTX_PARSORBLS |
| ctx_parstriangularis | TOT_CTX_PARSTRNGLS |
| ctx_pericalcarine | TOT_CTX_PERICLCRN |
| ctx_postcentral | TOT_CTX_POSTCNTRL |
| ctx_posteriorcingulate | TOT_CTX_POSTCNG |
| ctx_precentral | TOT_CTX_PRECNTRL |
| ctx_precuneus | TOT_CTX_PRECUNEUS |
| ctx_rh_bankssts | R_CTX_SSTSBANK |
| ctx_rh_caudalanteriorcingulate | R_CTX_CAUDANTCNG |
| ctx_rh_caudalmiddlefrontal | R_CTX_CAUDMIDFRN |
| ctx_rh_corpuscallosum | R_CTX_CRPCLM |
| ctx_rh_cuneus | R_CTX_CUNEUS |
| ctx_rh_entorhinal | R_CTX_ENTORHINAL |
| ctx_rh_frontalpole | R_CTX_FRNPOLE |
| ctx_rh_fusiform | R_CTX_FUSIFORM |
| ctx_rh_inferiorparietal | R_CTX_INFPRTL |
| ctx_rh_inferiortemporal | R_CTX_INFTEMP |
| ctx_rh_insula | R_CTX_INSULA |
| ctx_rh_isthmuscingulate | R_CTX_ISTHMUSCNG |
| ctx_rh_lateraloccipital | R_CTX_LATOCC |
| ctx_rh_lateralorbitofrontal | R_CTX_LATORBFRN |
| ctx_rh_lingual | R_CTX_LINGUAL |
| ctx_rh_medialorbitofrontal | R_CTX_MEDORBFRN |
| ctx_rh_middletemporal | R_CTX_MIDTMP |
| ctx_rh_paracentral | R_CTX_PARACNTRL |
| ctx_rh parahippocampal | R_CTX_PARAHPCMPL |
| ctx_rh_parsopercularis | R_CTX_PARSOPRCLRS |
| ctx_rh_parsorbitalis | R_CTX_PARSORBLS |
| ctx_rh_parstriangularis | R_CTX_PARSTRNGLRS |
| ctx_rh_pericalcarine | R_CTX_PERICLCRN |
| ctx_rh_postcentral | R_CTX_POSTCNTRL |
| ctx_rh_posteriorcingulate | R_CTX_POSTCNG |
| ctx_rh_precentral | R_CTX_PRECNTRL |
| ctx_rh_precuneus | R_CTX_PRECUNEUS |
| ctx_rh_rostralanteriorcingulate | R_CTX_ROSANTCNG |
| ctx_rh_rostralmiddlefrontal | R_CTX_ROSMIDFRN |
| ctx_rh_superiorfrontal | R_CTX_SUPERFRN |
| ctx_rh_superiorparietal | R_CTX_SUPERPRTL |
| ctx_rh_superiortemporal | R_CTX_SUPERTMP |

| | |
|-------------------------------|--------------------|
| ctx_rh_supramarginal | R_CTX_SUPRAMRGNL |
| ctx_rh_temporalpole | R_CTX_TMPPOLE |
| ctx_rh_transversetemporal | R_CTX_TRANSTMP |
| ctx_rostralanteriorcingulate | TOT_CTX_ROSANTCNG |
| ctx_rostralmiddlefrontal | TOT_CTX_ROSMIDFRN |
| ctx_superiorfrontal | TOT_CTX_SUPERFRN |
| ctx_superiorparietal | TOT_CTX_SUPERPRTL |
| ctx_superiortemporal | TOT_CTX_SUPERTMP |
| ctx_supramarginal | TOT_CTX_SUPRAMRGNL |
| ctx_temporalpole | TOT_CTX_TMPPOLE |
| ctx_transversetemporal | TOT_CTX_TRANSTMP |
| GR_FS | TOTFS_GYREC |
| Hippocampus | TOT_HIPPOCAMPUS |
| Left_Accumbens_area | L_ACCUMBENS |
| Left_Amygdala | L_AMYGDALA |
| Left_Caudate | L_CAUD |
| Left_Cerebellum_Cortex | L_CTX_CBLL |
| Left_Cerebellum_White_Matter | L_WM_CBLL |
| Left_choroid_plexus | L_CHORPLEX |
| Left_Hippocampus | L_HIPPOCAMPUS |
| Left_Pallidum | L_PALLIDUM |
| Left_Putamen | L_PUTAMEN |
| Left_Substantia_Nigra | L_SUBSTNCA_NGRA |
| Left_Thalamus_Proper | L_THALAMUS |
| Left_UnsegmentedWhiteMatter | L_WM_UNSEGMENTED |
| Left_VentralDC | L_VENTRALDC |
| OCC_FS | TOTFS_OCC |
| Pallidum | TOT_PALLIDUM |
| PREF_FS | TOTFS_PREFRN |
| Putamen | TOT_PUTAMEN |
| Right_Accumbens_area | R_ACCUMBENS |
| Right_Amygdala | R_AMYGDALA |
| Right_Caudate | R_CAUD |
| Right_Cerebellum_Cortex | R_CTX_CBLL |
| Right_Cerebellum_White_Matter | R_WM_CBLL |
| Right_choroid_plexus | R_CHORPLEX |
| Right_Hippocampus | R_HIPPOCAMPUS |
| Right_Pallidum | R_PALLIDUM |
| Right_Putamen | R_PUTAMEN |
| Right_Substantia_Nigra | R_SUBSTNCA_NGRA |
| Right_Thalamus_Proper | R_THALAMUS |
| Right_UnsegmentedWhiteMatter | R_WM_UNSEGMENTED |
| Right_VentralDC | R_VENTRALDC |
| Substantia_Nigra | TOT_SUBSTNCA_NGRA |
| TEMP_FS | TOTFS_TMP |
| Thalamus_Proper | TOT_THALAMUS_PRPR |
| UnsegmentedWhiteMatter | TOT_WM_UNSEGMENTED |
| VentralDC | TOT_VENTRALDC |
| wm_bankssts | TOT_WM_SSTSBNK |
| wm_caudalanteriorcingulate | TOT_WM_CAUDANTCNG |
| wm_caudalmiddlefrontal | TOT_WM_CAUDMIDFRN |
| wm_corpuscallosum | TOT_WM_CRPCLM |
| wm_cuneus | TOT_WM_CUNEUS |
| wm_entorhinal | TOT_WM_ENTORHINAL |
| wm_frontalpole | TOT_WM_FRNPOLE |
| wm_fusiform | TOT_WM_FUSIFORM |
| wm_inferiorparietal | TOT_WM_INFERPRTL |
| wm_inferiortemporal | TOT_WM_INFERTMP |
| wm_insula | TOT_WM_INSULA |
| wm_isthmuscingulate | TOT_WM_ISTHMUSCNG |
| wm_lateraloccipital | TOT_WM_LATOCC |
| wm_lateralorbitofrontal | TOT_WM_LATORBFRN |
| wm_lh_bankssts | L_WM_SSTSBANK |

| | |
|--------------------------------|--------------------|
| wm_lh_caudalanteriorcingulate | L_WM_CAUDANTCNG |
| wm_lh_caudalmiddlefrontal | L_WM_CAUDMIDFRN |
| wm_lh_corpuscallosum | L_WM_CRPCLM |
| wm_lh_cuneus | L_WM_CUNEUS |
| wm_lh_entorhinal | L_WM_ENTORHINAL |
| wm_lh_frontalpole | L_WM_FRNPOLE |
| wm_lh_fusiform | L_WM_FUSIFORM |
| wm_lh_inferiorparietal | L_WM_INFPRTL |
| wm_lh_inferiortemporal | L_WM_INFTMP |
| wm_lh_insula | L_WM_INSULA |
| wm_lh_isthmuscingulate | L_WM_ISTHMUSCNG |
| wm_lh_lateraloccipital | L_WM_LATOCC |
| wm_lh_lateralorbitofrontal | L_WM_LATORBFRN |
| wm_lh_lingual | L_WM_LINGUAL |
| wm_lh_medialorbitofrontal | L_WM_MEDORBFRN |
| wm_lh_middletemporal | L_WM_MIDTMP |
| wm_lh_paracentral | L_WM_PARACNTRL |
| wm_lh parahippocampal | L_WM_PARAHPCMPL |
| wm_lh_parsopercularis | L_WM_PARSOPRCLRS |
| wm_lh_parsorbitalis | L_WM_PARSORBLS |
| wm_lh_parstriangularis | L_WM_PARSTRIANGLRS |
| wm_lh_pericalcarine | L_WM_PERICLCRN |
| wm_lh_postcentral | L_WM_POSTCNTRL |
| wm_lh_posteriorcingulate | L_WM_POSTCNG |
| wm_lh_precentral | L_WM_PRECNTRL |
| wm_lh_precuneus | L_WM_PRECUNEUS |
| wm_lh_rostralanteriorcingulate | L_WM_ROSANTCNG |
| wm_lh_rostralmiddlefrontal | L_WM_ROSMIDFRN |
| wm_lh_superiorfrontal | L_WM_SUPERFRN |
| wm_lh_superiorparietal | L_WM_SUPERPRTL |
| wm_lh_superiortemporal | L_WM_SUPERTMP |
| wm_lh_supramarginal | L_WM_SUPRAMRGNL |
| wm_lh_temporalpole | L_WM_TMPPOLE |
| wm_lh_transversetemporal | L_WM_TRANSTMP |
| wm_lingual | TOT_WM_LINGUAL |
| wm_medialorbitofrontal | TOT_WM_MEDORBFRN |
| wm_middletemporal | TOT_WM_MIDTMP |
| wm_paracentral | TOT_WM_PARACNTRL |
| wm parahippocampal | TOT_WM_PARAHPCMPL |
| wm_parsopercularis | TOT_WM_PARSOPRCLRS |
| wm_parsorbitalis | TOT_WM_PARSORBLS |
| wm_parstriangularis | TOT_WM_PARSTRNGLRS |
| wm_pericalcarine | TOT_WM_PERICLCRN |
| wm_postcentral | TOT_WM_POSTCNTRL |
| wm_posteriorcingulate | TOT_WM_POSTCNG |
| wm_precentral | TOT_WM_PRECNTRL |
| wm_precuneus | TOT_WM_PRECUNEUS |
| wm_rh_bankssts | R_WM_SSTSBANK |
| wm_rh_caudalanteriorcingulate | R_WM_CAUDANTCNG |
| wm_rh_caudalmiddlefrontal | R_WM_CAUDMIDFRN |
| wm_rh_corpuscallosum | R_WM_CRPCLM |
| wm_rh_cuneus | R_WM_CUNEUS |
| wm_rh_entorhinal | R_WM_ENTORHINAL |
| wm_rh_frontalpole | R_WM_FRNPOLE |
| wm_rh_fusiform | R_WM_FUSIFORM |
| wm_rh_inferiorparietal | R_WM_INFERIORPRTL |
| wm_rh_inferiortemporal | R_WM_INFERIORTMP |
| wm_rh_insula | R_WM_INSULA |
| wm_rh_isthmuscingulate | R_WM_ISTHMUSCNG |
| wm_rh_lateraloccipital | R_WM_LATOCC |
| wm_rh_lateralorbitofrontal | R_WM_LATORBFRN |
| wm_rh_lingual | R_WM_LINGUAL |
| wm_rh_medialorbitofrontal | R_WM_MEDORBFRN |

| | |
|--------------------------------|-------------------|
| wm_rh_middletemporal | R_WM_MIDTMP |
| wm_rh_paracentral | R_WM_PARACNTRL |
| wm_rh_parahippocampal | R_WM_PARAHPCMPL |
| wm_rh_parsopercularis | R_WM_PARSOPRCLRS |
| wm_rh_parsorbitalis | R_WM_PARSORBLS |
| wm_rh_parstriangularis | R_WM_PARSTRNGLRS |
| wm_rh_pericalcarine | R_WM_PERICLCRN |
| wm_rh_postcentral | R_WM_POSTCNTRL |
| wm_rh_posteriorcingulate | R_WM_POSTCNG |
| wm_rh_precentral | R_WM_PRECNTRL |
| wm_rh_precuneus | R_WM_PRECUNEUS |
| wm_rh_rostralanteriorcingulate | R_WM_ROSANTCNG |
| wm_rh_rostralmiddlefrontal | R_WM_ROSMIDFRN |
| wm_rh_superiorfrontal | R_WM_SUPERFRN |
| wm_rh_superiorparietal | R_WM_SUPERPRTL |
| wm_rh_superiortemporal | R_WM_SUPERTMP |
| wm_rh_supramarginal | R_WM_SUPRAMRGNL |
| wm_rh_temporalpole | R_WM_TMPPOLE |
| wm_rh_transversetemporal | R_WM_TRANSTMP |
| wm_rostralanteriorcingulate | TOT_WM_ROSANTCNG |
| wm_rostralmiddlefrontal | TOT_WM_ROSMIDFRN |
| wm_superiorfrontal | TOT_WM_SUPERFRN |
| wm_superiorparietal | TOT_WM_SUPERPRTL |
| wm_superiortemporal | TOT_WM_SUPERTMP |
| wm_supramarginal | TOT_WM_SUPRAMRGNL |
| wm_temporalpole | TOT_WM_TMPPOLE |
| wm_transversetemporal | TOT_WM_TRANSTMP |
| MCBP | TOT_CORTMEAN |

REFERENCES

1. Gorgolewski, K.J., et al. The brain imaging data structure, a format for organizing and describing outputs of neuroimaging experiments. *Sci Data* 2016; 3:160044. PMID: 27326542 PMCID: PMC4978148 DOI: 10.1038/sdata.2016.44.
2. Chien DT, Bahri S, Szardenings AK, Walsh JC, Mu F, Su M-Y, et al. Early Clinical PET Imaging Results with the Novel PHF-Tau Radioligand [F-18]-T807. *J. Alzheimer's Dis.* 2013; 34: 457–468.
3. Eisenstein, S.A., Koller, J.M., Piccirillo, M., Kim, A., Antenor-Dorsey, J.A., Videen, T.O., Snyder, A.Z., Karimi, M., Moerlein, S.M., Black, K.J., Perlmutter, J.S., Hershey, T., 2012. Characterization of extrastriatal D2 in vivo specific binding of [(1)(8)F](N-methyl)benperidol using PET. *Synapse* 66, 770-780.
4. Fischl B. FreeSurfer. *NeuroImage* 2012; 62(2):774-781. PMCID: PMC: 222857
5. Frouin V, Comtat C, Reilhac A, Grégoire MC. Correction of Partial-Volume Effect for PET Striatal Imaging: Fast Implementation and Study of Robustness. *J Nucl Med* 2002; 43:1715–1726
6. Hajnal, J.V., Saeed, N., Soar, E.J., Oatridge, A., Young, I.R., Bydder, G.M., 1995. A registration and interpolation procedure for subvoxel matching of serially acquired MR images. *J Comput Assist Tomogr* 19, 289-296.
7. Joshi, A., Koeppe, R.A., Fessler, J.A., 2009. Reducing between scanner differences in multi-center PET studies. *Neuroimage* 46, 154-159.
8. Klunk WE, Engler H, Nordberg A, Wang, Y, Blomqvist G, Holt DP, Bergstrom M, Savitcheva I, Huang GF, Estrada S, Ausen B, Debnath ML, Barletta J, Price JC, Sandell J, Lopresti BJ, Wall A, Koivisto P, Antoni G, Mathis CA, Langstrom B. Imaging brain amyloid in Alzheimer's disease with Pittsburgh Compound-B. *Ann Neurol* 2004; 55, 306-319.
9. Klunk WE, Koeppe RA, Price JC, Benzinger TL, Devous MD Sr, Jagust WJ, Johnson KA, Mathis CA, Minhas D, Pontecorvo MJ, Rowe CC, Skovronsky DM, Mintun MA. The Centiloid Project: Standardizing quantitative amyloid plaque estimation by PET. *Alzheimer's & Dementia* 2015; 11(1):1-15.e4.
10. Logan J, Fowler AH, Volkow ND. Distribution volume ratios without blood sampling from graphical analysis of PET data. *J Cereb Blood Flow Metab* 1996; 16:834–840.
11. Lopresti BJ, Klunk WE, Mathis CA, Hoge JA, Ziolkowski SK, Lu X, Meltzer CC, Schimmel K, Tsopelas ND, DeKosky ST, Price JC. Simplified quantification of Pittsburgh Compound B amyloid imaging PET studies: a comparative analysis. *J Nucl Med* 2005; 46:1959-1972.
12. Marcus, DS, Archie, KA, Olsen, T, Ramaratnam, M. The open source neuroimaging research enterprise. *J. Digital Imaging* 2007; 20:130-138.
13. McCormick LM, Ziebell S, Nopoulos P, Cassell M, Andreasen NC, Brumm M. Anterior Cingulate Cortex: An MRI-based parcellation method. *NeuroImage* 2006; 32:1167-1175.
14. Mintun MA, LaRossa GN, Sheline YI, Dence CS, Lee SY, Mach RH, Klunk WE, Mathis CA, DeKosky ST, Morris JC. [11C]PIB in a nondemented population: Potential antecedent marker of Alzheimer disease. *Neurology* 2006; 67:446-452
15. Shruti, M, Gordon BA, Su, Y, Christensen, J, Friedrichsen, K, Jackson K, Hornbeck, R, Balota DM, Cairns, N, Ances, B, Morris, JC. Benzinger TLS. Tau PET imaging in preclinical Alzheimer's Disease: Classifying tau Positivity. *NeuroImage* 2017; 161: 171-178
16. Morris, JC, Roe, CM, Xiong, C, Fagan, AM, Goate, AM, Holtzman, DM, Mintun, MA. APOE predicts amyloid-beta but not tau Alzheimer pathology in cognitively normal aging. *Ann Neurol* 2010; 67:122-131.
17. Ostrowitzki S, Deptula D, Thurfjell L, Barkhof F, Bohrmann B, Brooks DJ, Klunk WE, Ashford E, Yoo K, Xu ZX, Loetscher H, Santarelli L. Mechanism of amyloid removal in patients with Alzheimer disease treated with gantenerumab. *Arch Neurol* 2011; 69:198-207

18. Price TR, Manolio TA, Kronmal RA, Kittner SJ, Yue NC, Robbins J, Anton-Culver H, O'Leary DH. Silent brain infarction on magnetic resonance imaging and neurological abnormalities in community-dwelling older adults. The Cardiovascular Health Study. CHS Collaborative Research Group. *Stroke*. 1997;28(6):1158-64. PMID: 9183343.
19. Robb, R.A., Hanson, D.P., Karwoski, R.A., Larson, A.G., Workman, E.L., Stacy, M.C. Analyze: a comprehensive, operator-interactive software package for multidimensional medical image display and analysis. *Comput Med Imaging Graph* 1989; 13:433-454.
20. Rousset O, Ma Y, Evans A. Correction for partial volume effects in PET: principle and validation. *J Nucl Med* 1998; 39:904–11.
21. Rousset O, Zaidi H. Correction of partial volume effects in emission tomography. In: Zaidi H, editor. *Quantitative analysis of nuclear medicine images*. New York: Springer; 2006. p. 236–271.
22. Rowland DJ, Garbow JR, Laforest R, Snyder AZ. 2005 Registration of [18F]FDG microPET and small-animal MRI. *Nucl Med Biol* 2005; 32:567-72
23. Sperling RA, Aisen PS, Beckett LA, Bennett DA, Craft S, Fagan AM, Iwatsubo T, Jack CR, Jr., Kaye J, Montine TJ, Park DC, Reiman EM, Rowe CC, Siemers E, Stern Y, Yaffe K, Carrillo MC, Thies B, Morrison-Bogorad M, Wagster MV, Phelps CH. Toward defining the preclinical stages of Alzheimer's disease: recommendations from the National Institute on Aging-Alzheimer's Association workgroups on diagnostic guidelines for Alzheimer's disease. *Alzheimer's & dementia*. 2011;7(3):280-92. PMID: 21514248; PMCID: PMC3220946
24. Su Y, D'Angelo GM, Vlassenko AG, Zhou GF, Snyder AZ, Marcus DS, et al. Quantitative Analysis of PiB-PET with FreeSurfer ROIs. *PLoS One* 2013;8(11):e73377. PMCID: 3819320
25. Su Y, Blazey TM, Snyder AZ, Raichle ME, Marcus DS, Ances BM, Bateman RJ, Cairns NJ, Aldea P, Cash L, Christensen JJ, Friedrichsen K, Hornbeck RC, Farrar AM, Owen CJ, Mayeux R, Brickman AM, Klunk W, Price JC, Thompson PM, Ghetti B, Saykin AJ, Sperling RA, Johnson KA, Schofield PR, Buckles V, Morris JC, Benzinger TL, Network DIA. Partial volume correction in quantitative amyloid imaging. *Neuroimage*. 2015;107:55-64. PMCID: 4300252.
26. Su Y, Blazey TM, Owen CJ, Christensen JJ, Friedrichsen K, Joseph-Mathurin N, Wang Q, Hornbeck RC, Ances BM, Snyder AZ, Cash LA, Koeppe RA, Klunk WE, Galasko D, Brickman AM, McDade E, Ringman JM, Thompson PM, Saykin AJ, Ghetti B, Sperling RA, Johnson KA, Salloway SP, Schofield PR, Masters CL, Villemagne VL, Fox NC, Forster S, Chen K, Reiman EM, Xiong C, Marcus DS, Weiner MW, Morris JC, Bateman RJ, Benzinger TL, Dominantly Inherited Alzheimer N. Quantitative Amyloid Imaging in Autosomal Dominant Alzheimer's Disease: Results from the DIAN Study Group. *PLoS One*. 2016;11(3):e0152082. PMCID: PMC4807073.
27. Su Y, Flores S, Hornbeck RC, Speidel B, Vlassenko AG, Gordon BA, Koeppe RA, Klunk WE, Xiong C, Morris JC, Benzinger TLS. Utilizing the Centiloid scale in cross-sectional and longitudinal PiB PET studies. *NeuroImage: Clinical* 19 (2018): 406-416.
28. Su Y, Flores S, Wang G, et al. Comparison of Pittsburgh compound B and florbetapir in cross-sectional and longitudinal studies. *Alzheimers Dement (Amst)*. 2019;11:180–190.
29. Talairach J, Tournoux P. Co-planar Stereotaxic Atlas of the Human Brain: 3-D Proportional System: An Approach to Cerebral Imaging. Stuttgart, Germany: Thieme Medical Publishers; 1988.
30. Wahlund LO, Barkhof F, Fazekas F, Bronge L, Augustin M, Sjogren M, Wallin A, Ader H, Leys D, Pantoni L, Pasquier F, Erkinjuntti T, Scheltens P. A new rating scale for age-related white matter changes applicable to MRI and CT. *Stroke*. 2001;32(6):1318-22. PMID: 11387493.
31. Accorsi R, Adam LE, Werner ME, and Karp JS. Optimization of a fully 3D single scatter algorithm for 3D PET. *Phys Med Bio* 2004; 49: 2577-2598.